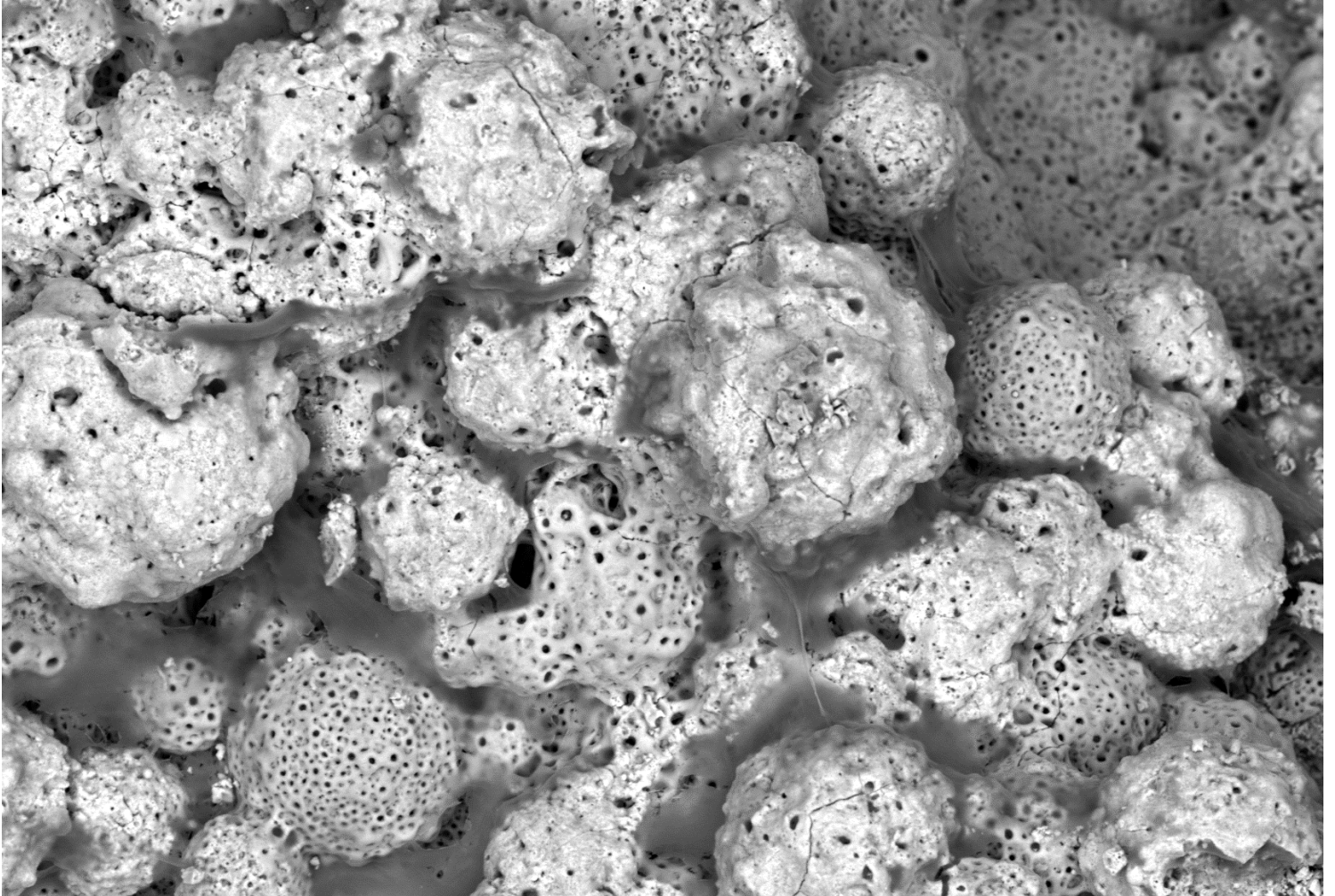


MSc Thesis

Osteogenic and angiogenic properties of strontium incorporated titanium implants

Francisca Gelderman



28-08-2018

Supervisors: Dr. ir. E.L. Fratila-Apachitei

Dr. ir. I. Apachitei.

I.A.J. van Hengel

Dr. B.C.J. van der Eerden

 TU Delft

Osteogenic and angiogenic properties of strontium incorporated titanium implants

By

Francisca Gelderman (4614739)

In partial fulfilment of the requirements for the degree of

Master of Science

in Biomedical Engineering

at the Delft University of Technology,

to be defended publically on 28-08-2018, 13:00.

Supervisors: Dr. ir. L. Fratilla-Apachitei

Dr. ir. I. Apachitei

Ir. I.A.J van Hengel

Dr. B.C.J. van der Eerden

Prof. dr. A.A. Zadpoor

Biomaterials and Tissue Biomechanics Section

Biomechanical Engineering Department

Faculty of Mechanical, Maritime and Materials Engineering

Delft University of Technology

An electronic version of this thesis is available at <http://repository.tudelft.nl/>.

Abstract

In the current day and age, osteogenic bone implants are important to reduce healing time and infections after bone implantation. To help induce bone formation, the implant surface can be biofunctionalized with different agents. A promising surface modification technique used to treat titanium implants is Plasma Electrolytic Oxidation (PEO). In previous research, strontium has shown to be a bone inducing agent, both in implant surfaces and in culture by stimulating mesenchymal stem cells (MSCs) to form bone. To explore this technique and its merits further, the effect of strontium and PEO combined was investigated by looking at the effect of strontium and strontium-incorporated implants on the viability, metabolic activity and osteogenic differentiation of human MSCs. In these experiments a 1 hour seeding time and 2 hour seeding time group were assessed, in which the cells were able to attach to the implant for 1 or 2 hours in a cell immersion, after which the implants with only the attached cells were cultured further. The implants groups were, based on the strontium concentration in the electrolyte, NT (not treated with PEO), PT, PT + 0.3 M Sr, PT + 0.5 M Sr and PT + 1 M Sr. The effects of strontium on the mutual effects of MSCs and endothelial cells (ECs) were also investigated, since the interaction of these cells is vital in the formation of blood vessels. To investigate these two topics, firstly 5 types of implants surfaces were created and their characteristics were analyzed. Then the effects of these implants on viability, metabolic activity and differentiation of MSCs were assessed. The results showed an increasing viability of MSCs on implants with strontium incorporated into them. Metabolic activity and differentiation improved in MSCs on the two medium strontium concentration incorporated implants, although there were differences between different seeding times of MSCs. Due to differences in morphology of the strontium incorporated implants, and presumably the oxide layer thickness, these results could both be the result of these material characteristics and/or of the strontium release of the implants. In future experiments, the implant characteristics must be created more similarly, so the effect of the single variable strontium can be assessed. Concerning the effects of strontium on the mutual effects of MSCs and ECs, co-culture with MSCs decreased the gene expression of VEGF-A, a marker of early angiogenesis.

Table of contents

Abstract.....	3
1. Introduction	6
2. Materials and methods	8
2.1. Study design.....	8
2.2. Design and fabrication of implants	8
2.3. Synthesis of multifunctional surface by plasma electrolytic oxidation	9
2.3.1. Plasma electrolytic oxidation set-up.....	9
2.3.2. Preparation of electrolytes for plasma electrolytic oxidation	9
2.3.3. Synthesis of multifunctional TiO ₂ layers by plasma electrolytic oxidation.....	10
2.4. Biomaterial characterization.....	10
2.4.1. Implant surface characterization	10
2.4.1. Ion release profile	10
2.5. In-vitro tests.....	11
2.5.1 Experiments with MSCs on implants	11
2.5.2 Experiments with MSCs and ECs in co-culture.....	12
2.5.3. Live/dead assay.....	13
2.5.4. Cell morphology characterization.....	14
2.5.5. Cell viability and proliferation assay	14
2.5.6. Alkaline phosphate assay.....	15
2.5.7. BCA assay	17
2.5.8. qRT-PCR.....	18
2.6 Statistics	19
3. Results	20
3.1 Biomaterial synthesis.....	20
3.1.1. Voltage-time response of plasma electrolytic oxidation treatment.....	20
3.2. Biomaterial Characterization	21
3.2.1 Surface morphology of implants after plasma electrolytic oxidation treatment	21
3.2.1 Ion release profile of implants	22
3.3. In-vitro tests.....	22
3.3.1 In-vitro experiments on MSCs implants.....	22
3.3.1.1. Cell morphology of MSCs on implants.....	22
3.3.1.2. Viability of MSCs on implants	25

3.3.1.3. Metabolic activity of MSCs on implants	25
3.3.1.4. Differentiation of MSCs on implants.....	26
3.3.2. Co-cultures of MSCs and ECs with strontium	28
3.3.2.1. Metabolic activity of MSCs and ECs in co-culture with strontium.....	28
3.3.2.2. Differentiation of MSCs in co-culture with ECs and strontium.....	29
3.3.2.3. Differentiation of ECs in co-culture with MSCs and strontium.....	30
4. Discussion.....	30
4.1 Implant characteristics resulting from the PEO process.....	31
4.2 1 hour vs 2 hours seeding time.....	32
4.3 Co-culture vs single culture response to strontium.....	33
5. Conclusion.....	34
6. Acknowledgements.....	35
7. References	36
8. Appendix	39
8.1 Effects of Strontium in medium.....	39
8.2 Effect of ECM coating of implants of MSCs.....	41
8.3 SEM images of MSCs on implants.....	42
8.4 Release of strontium in molars.....	44
8.5 Primer sequences for PCR.....	45

1. Introduction

Aging of the population presents a major challenge in modern healthcare. As the population ages, the number of chronic health problems increases steadily. One of the most common chronic health issues is osteoarthritis (OA), a bone and joint disease that will eventually lead to replacement of the joint by an implant. Approximately 1-3% of the elderly population will need a hip arthroplasty in their life [1]. Due to the ever increasing life-expectancy, total costs associated with OA—related operations will rise. Besides the aging of the population, it is estimated that 12% of all primary hip implantations need a revision, which will greatly increase the healthcare costs [2].

Thirty percent of total knee revisions and 55% of total hip revisions are caused by loosening of the bone implants [3, 4]. All the revisions can lead to bone loss, which complicates the replacement and increases the need for accelerated anchoring of the implant [5]. Good ingrowth of bone tissue into the implant (osseointegration) can reduce loosening of implants and increase stability of the joint [6]. Improving osseointegration is therefore a primary objective of orthopedic implants.

Proper fixation between bone and implants requires osseointegration, including a good blood supply. Therefore, fast bone formation and ingrowth into the implant and no adverse effects on the blood vessel forming cells, endothelial cells (ECs), are crucial. In bone (in)growth and remodeling, three cell types are directing bone formation and resorption: osteoblasts, osteoclasts and osteocytes. Osteocytes are by far the most numerous and are mechanical force sensing cells that determine whether more or less bone mass is needed based on mechanical stimuli. Osteocytes signal to osteoblasts for bone formation and osteoclasts for bone resorption. Osteoblasts are derived from mesenchymal stem cells (MSCs) that reside in the bone marrow. Bone remodeling, the process of osteoclast-driven resorption, followed by osteoblast-mediated bone formation is taking place throughout life to respond to microdamages in bones in order to keep the skeleton healthy [7].

Apart from bone remodeling, bone regeneration also depends on the activity of osteoblasts and osteoclasts, yet with the aim to restore larger bone defects. Placement of a bone implant resembles such a situation where bone regeneration is needed. In a situation like this, after damage, blood accumulates at the site of damage [8, 9]. The blood starts clotting within a few hours as a result of constricting blood vessels and a blood clot or hematoma forms. The immune cells from the blood induce inflammation in the area and recruit MSCs and chondrocytes to the wound area and increase osteoblast and chondrocyte differentiation and the formation of a callus: a temporarily formed calcified tissue to stabilize the surrounding area, which will later be remodeled into bone. The immune cells and the lack of oxygen also induce endothelial cell morphogenesis and blood vessel formation (angiogenesis) in the area [7]. This type of blood vessel formation called sprouting angiogenesis, is characterized by outgrowth of endothelial cells, which grow towards an angiogenic stimulus [10]. The chondrocytes are responsible for the process called endochondral ossification, in which mineralized cartilage is formed, which is eventually replaced by bone. A good bone implant is composed of materials that enhance these processes.

Porous titanium implants are widely used to replace joints, specifically in dental implantations, acetabular cups and femoral stems in hip implants and in tibial parts of knee implants [11]. Porous structures can be made using additive manufacturing, for example by selective laser melting. This technique has the advantage of creating highly porous structures with a very high accuracy. The most universally applied alloy in orthopedic implants and selective laser melting is the Ti6Al4V alloy consisting

of titanium, aluminum and vanadium, as it has the most appropriate material properties: the modulus of elasticity is favorable, just like the tensile, compressive and shear strength. The hardness and toughness are close to those of human bones for a metal, which prevents mechanical issues such as stress shielding and implant fractures [12]. One of the properties that makes titanium such an attractive material, is its inertness in the human body. The inert properties of titanium are caused by the oxidized outer layer that forms naturally [13]. The surface provides an excellent means for modification to promote rapid osseointegration [13-15].

One of the more recently discovered agents that promote osseointegration is strontium. Strontium has already been used as an oral treatment as an additive treatment to bone implant placement *in vivo* [13, 16]. Strontium has various mechanisms of action. One of the mechanisms through which strontium stimulates bone formation is the calcium sensing receptor (CaSR), a protein that can be activated by both calcium and strontium, due to their similarity [17, 18]. Besides bone anabolic effects, strontium inhibits osteoclast activity by increasing osteoprotegerin (OPG) and decreasing the receptor activator of nuclear factor kappa B ligand (RANKL) expression by osteoblasts, both resulting in less bone resorption [17]. Strontium also improves angiogenesis *in vitro* [19]. Directly incorporated strontium in the surface of bone implants could thus improve osseointegration.

The surface of implants can help the bone regeneration process by providing a scaffold made of materials that promote MSC differentiation towards osteoblasts. A new and promising surface modification method is plasma electrolytic oxidation (PEO), also called micro-arc oxidation (MAO), in which the outer layer titanium oxide is expanded. During this treatment, high potentials are employed that cause discharges. The resulting plasma remodels the structure of the oxide layer on the titanium, which causes the formation of many interconnected micropores. This treatment can be used to grow thick, crystalline oxide layers with a high hardness, wear and corrosion resistance [20]. Compared to other surface modification techniques, metal surfaces are highly customizable with PEO treatment that enables various pore sizes by changing the peak current. Furthermore, PEO is suitable for highly porous structures and lasts only 5 minutes. Finally, PEO treatment of implants provides a means to include active surface components, such as calcium and phosphate, which are both natural ingredients of bone crystals (hydroxyapatite) that improve attachment to the surface, and strontium.

Research into the combination of titanium implants and PEO-incorporated strontium, especially in combination with human cells has hardly been investigated. Therefore, this project has applied PEO to incorporate strontium into the surface of Ti6Al4V selective laser melted implants, and for the first time, assess the effects of these implants on the viability, metabolic activity and differentiation of healthy adult MSCs. The aim was to produce implants that release strontium ions, determine the range of release and to assess the effects of MSCs. Additionally, the influence of strontium on angiogenesis was assessed in co-cultures of endothelial cells and mesenchymal stem cells. The aim was to assess the mutual effects of MSCs and ECs on angiogenesis and osteogenesis and to test the influence of strontium on these co-cultures.

2. Materials and methods

2.1. Study design

In **Table 1** an overview is given of the design, synthesis and characterization methods that were used in this study.

Table 1: Study Design

Study stage	Subcategory	Methods
Implant synthesis and biofunctionalization	Implant synthesis	Selective laser melting (SLM)
	Surface biofunctionalization	Plasma Electrolytic Oxidation (PEO)
Surface characterization	Surface morphology	Scanning Electron Microscopy (SEM)
	Strontium ion release	Inductively coupled plasma optical emission spectrometry (ICP-OES)
<i>In vitro</i> testing of MSCs and ECs	Cell morphology	Scanning Electron Microscopy (SEM)
	Proliferation	Presto Blue assay
	Viability	Live Dead staining
	Differentiation	ALP and BCA assay

2.2. Design and fabrication of implants

The implants used in this project were previously designed by van Hengel et al and the design is shown in **Figure 1** [20]. The implant was produced by selective laser melting of plasma-atomised Ti₆Al₄V powder (AP&C, Boisbriand, Quebec, Canada) [20, 21]. The aspect ratio of the implant is a number based on the ratio of the z-direction to z-direction of the original design, the surface area compared to solid wire is the fold increase in surface area compared to a solid wire and the porosity the amount of pores compared to a solid wire.

Aspect ratio (AR)	1.0
Surface area compared to solid wire	3.75
Porosity (%)	14.4

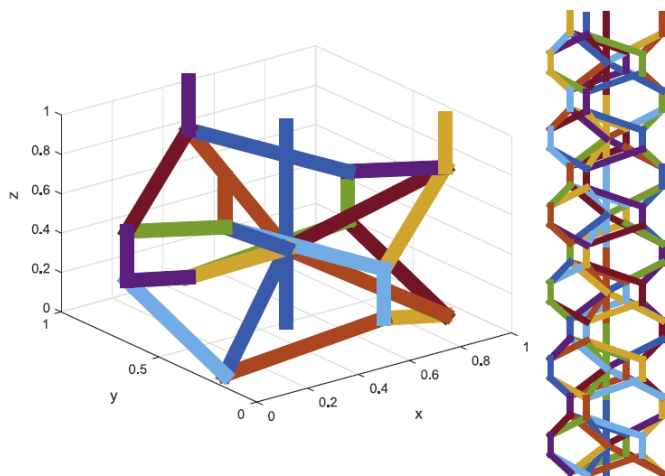


Figure 1: Previously designed implant by van Hengel et al [20]. Unit cell (left) and stacked unit cells resulting in wire-like implant (right).

2.3. Synthesis of multifunctional surface by plasma electrolytic oxidation

2.3.1. Plasma electrolytic oxidation set-up

The PEO set-up used to perform the PEO process in this project was custom made. The set-up consisted of an AC power supply (ACS 1500, ET Power Systems Ltd., Chesterfield, United Kingdom) connected with a computer interface through a data acquisition board (SCXI, National Instruments, Austin, USA). The electrolyte was held in a double-walled glass cylinder, which was continuously cooled by the cooling fluid (1:1 of ethylene glycol and water) using a thermostatic bath and pump (Thermo Haake V15, Thermo Electron, Massachusetts, USA). A thermometer was used to measure the temperature of the electrolyte at the beginning and end of the PEO process. In this set-up, the implants served as the anode and a cylindrical shaped stainless steel cathode was used.

2.3.2. Preparation of electrolytes for plasma electrolytic oxidation

To produce surfaces with different concentrations of strontium, 5 electrolytes with different chemical compositions were prepared to assess the effects of strontium on the biocompatibility of the additively manufactured implants. In all electrolytes, 0.02 M calcium glycerophosphate (CaGly) (Sigma Aldrich) and 0.16 M calcium acetate (CaA) (Sigma Aldrich) was present. These were prepared by adding 19.2 g calcium acetate and 3.36 g calcium glycerophosphate to 800 mL demineralized water. Additionally, various concentrations of strontium acetate (SrA) (Sigma Aldrich) were added, as shown in **Table 2**. In the table PT = PEO treated. All electrolytes were stirred at 500 rpm until the solution was clear. The PT + 0.1 M Sr group was only used in the pilot experiments.

Table 2: Chemical composition of electrolytes. PT: PEO treated

Abbreviation of electrolyte	Electrolyte composition		
	CaA (M)	CaGly (M)	SrA (M)
PT			
PT + 0.1 M Sr	0.16	0.02	0.1
PT + 0.3 M Sr	0.16	0.02	0.3
PT + 0.5 M Sr	0.16	0.02	0.5
PT + 1 M Sr	0.16	0.02	1

2.3.3. Synthesis of multifunctional TiO₂ layers by plasma electrolytic oxidation

Before fabrication of the surfaces by PEO, the electrolytes were cooled below 9°C using a thermostatic bath. 800 mL of electrolyte was used to fill the electrolytic cell that was stirred continuously through the PEO process at 500 rpm, to ensure a homogeneous distribution of the electrolyte. While waiting for the electrolyte to cool, non-treated implants (NT) were prepared by sonication in acetone for 5 minutes, sonication in 96% ethanol for 5 minutes, sonication in demineralized water for 5 minutes and air drying. After preparing the implants, the current density was set with an earlier PEO treated sample: a strontium incorporated-PEO treated sample for the PT + Sr groups and a sample with only CaA and CaGly in the electrolyte for the PT group. The current density applied to the implants was 20 A/dm² for 300 seconds at a current frequency of 50 Hz. While using the PEO electrolyte without strontium, 4 implants could be processed using a special set-up and a current density of 20 A/dm² was used, which approximated to 1556 mA. With the strontium-incorporated electrolyte, only one implant was processed due to the increasing resistance of the electrolyte with increasing concentrations of strontium. Therefore, while using an electrolyte with strontium, and using the same current density, the current approximates to 389 mA for 1 implant. The voltage-time transients were recorded every second using the National Instruments SCXI data acquisition system. After the PEO treatment, the implants were rinsed in running tap water for 1 minute, flushed with distilled water and subsequently air dried.

2.4. Biomaterial characterization

2.4.1. Implant surface characterization

To analyze the surface morphology of the implant, a scanning electron microscope (SEM) was used (JSM-IT100, Jeol, Tokyo, Japan). The secondary electron mode (SED) and backscattered electron modes (BEC) were used to image the implants using an electron beam with an acceleration voltage of 10 KeV and a probe current at 10 mm working distance to avoid charging. Pictures were taken at various magnifications: 2000x, 1500x, 1000x and 500x at one spot on the implant as well as 100x magnification over the whole length of an implant segment of 5 mm.

2.4.1. Ion release profile

The strontium ion release of the strontium-incorporated implants was analyzed by submerging 1.5 cm implants in 1 mL phosphate buffered saline (PBS) dark Eppendorf tubes which were kept at 37°C in a thermostatic bath, to mimic physiological conditions. The PBS was collected and refreshed after 12 hours and 1, 2, 4, 7, 14 and 28 days. The collected PBS was analyzed for strontium ion content using Inductive Coupled Plasma- Optical Emission Spectrometry (ICP-OES), using a spectrometer (Spectro Arcos, Kleve, Germany), which measures strontium content in parts per billion (mass fraction).

2.5. In-vitro tests

For all experiments, MSCs from a healthy adult donor from Lonza (donor 4266) and endothelial cells (ECs) using the cell line EA.hy926 were used. The EA.hy926 was created by fusing primary human umbilical vein cells (HUVECs) with A549 cells (a breast cancer cell line)[22]. Clones of this fusion were selected as the final cell line.

The *in vitro* studies consisted of two types of experiments. In the first type the effects of strontium incorporated implants on MSCs were assessed, while in the second type the effect of strontium on the cell-cell interactions of MSCs and ECs in co-culture were assessed.

2.5.1 Experiments with MSCs on implants

In the first type of experiments, implants were cut to pieces of 1 cm in length, put into PCR strips (Biorad 8 tube strip & cap, Biorad laboratories, USA) and sterilized by autoclaving them for 6 hours at 121 °C. After sterilization, 100 µL of a $1.5 \cdot 10^6$ MSCs/mL cell solution was seeded on each implant. The implants were then put in an incubator at 37°C, 5% CO₂ and 20% O₂. For 1 or 2 hours, the PCR strips with implants, that were placed horizontally, were turned around every 10 (1 hour seeding time) or 20 (2 hour seeding time) minutes. The implants were then transferred to a 48-wells plate (Greiner; Figure 2) with 200 µL DMEM (440 mL DMEM(including 4.5 g/L D-glucose, L-Glutamine + pyruvate), 10 mL Penicillin-Streptomycin (5000 U/mL Penicillin, 500 µg/mL Streptomycin, Thermo Fischer, Waltham, MA USA), 2.39 g 20 mM HEPES (H3375, Sigma Aldrich, Darmstadt, Germany) and 50 mL heat-inactivated fetal calf serum (FBS, 12306C, lot 0044M3395, Sigma Aldrich, Darmstadt, Germany) at pH 7.5 and sterilized through a 0.22 µm filter (Stericup QuickRelease, Milipore, Billerica, MA, USA).

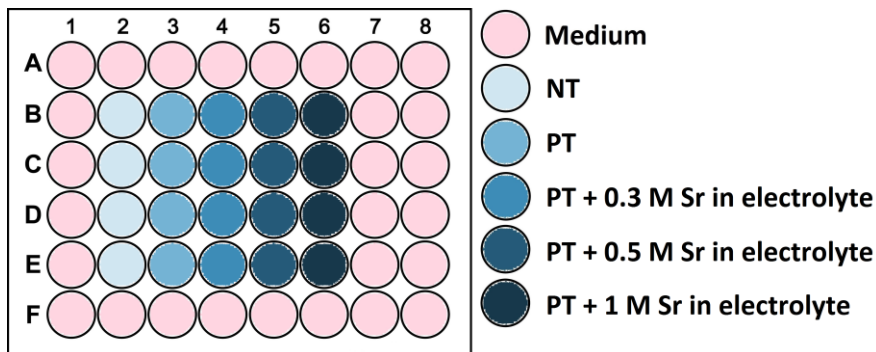


Figure 2: Plate layout of MSCs on implants, NT = non treated implants, PT = PEO treated implants

After 24 h, the implants were transferred to a new 48 wells plate with 200 µL DMEM per well, to reduce cell growth on the bottom of the well of MSCs that had previously fallen off the implant. 2 days after seeding, the differentiation of MSCs was initiated by adding osteogenic medium (DMEM as described before) + 100 nM dexamethasone (1:10,000 from 1 mM stock in ethanol (Sigma Aldrich, Darmstadt, Germany), 10 mM β-glycerophosphate (1:200 from stock 2M in H₂O) and 0.1 mM vitamin C (1:500 from 0.05 M stock in α-MEM). The day of differentiation initiation is called d0. On d3, d5, d7 and d14, a Presto Blue assay was done, as described in section 2.5.5. Cell viability and proliferation assay. On d0 a Live/Dead staining was done as described in section 2.5.3. Live/dead assay. On d5 or d7 and d10 and d14, an alkaline phosphatase (ALP) and bicinchoninic acid assay (BCA) assay were done as described in section 2.5.6. Alkaline phosphate assay and section 2.5.7. BCA assay, respectively. On d5 or d7 (depending on the experiment) and d10 and d14, implants with cells were washed with PBS and then

fixated with 200 μ L 4% paraformaldehyde (Sigma) and 1% glutaraldehyde (Merck, Darmstadt, Germany) in PBS per implant. The experimental timeline is also shown in **Figure 3**.

d-3	<i>Sterilization of implants</i>
d-2	<i>Seeding of MSCs on implants, SEM</i>
d0	<i>Initiation of differentiation, SEM, Live/Dead staining (2h)</i>
d3	<i>Presto Blue assay (2h), SEM (2h)</i>
d5	<i>Presto Blue assay</i>
d7	<i>Presto Blue assay (1h), ALP assay, BCA assay</i>
d10	<i>Presto Blue assay (2h)</i>
d11	<i>ALP assay (2h), BCA assay (2h), Presto Blue assay (2h)</i>
d14	<i>SEM (2h), ALP assay, BCA assay, Presto Blue assay (2h)</i>

Figure 3: Timeline of experiments on MSCs on implants, 1h = 1 hour seeding time 2h = 2 hours seeding time, d = day

2.5.2 Experiments with MSCs and ECs in co-culture

In the second type of experiments, MSCs were seeded in the top and bottom rows of wells in a 12-wells plate 3 days before the start of the co-culture with endothelial cells (d-3) with 700 μ L DMEM. After two days (d-1), differentiation of the MSCs was initiated with and without 1 mM strontium acetate. Endothelial cells (ECs) were seeded in transwells (ThinCerts, 0.4 μ m pore size, Greiner bio-one, Alphen aan den Rijn, the Netherlands) in the middle and bottom rows of wells in the same 12-wells plate (700 μ L DMEM in every well of a 12-well plate (under the transwell) + 500 μ L DMEM in every thinsert that is placed in each well). The upper row of thinserts contained only medium and served as a control. On day 0, the thinserts were refreshed with osteogenic differentiation medium with and without 1 mM

strontium acetate and then put into the 12-wells plate with MSCs. The plate layouts are shown in **Figure 4** and **Figure 5**. On day 2 a Presto Blue assay was done and on day 6 cell extracts were isolated for an ALP and BCA assay.

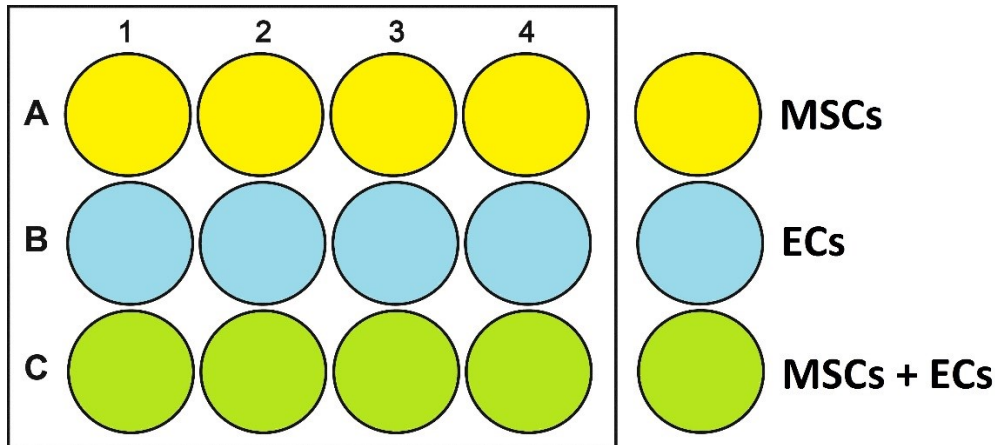


Figure 4: Layout of co-culture of MSCs and ECs - control

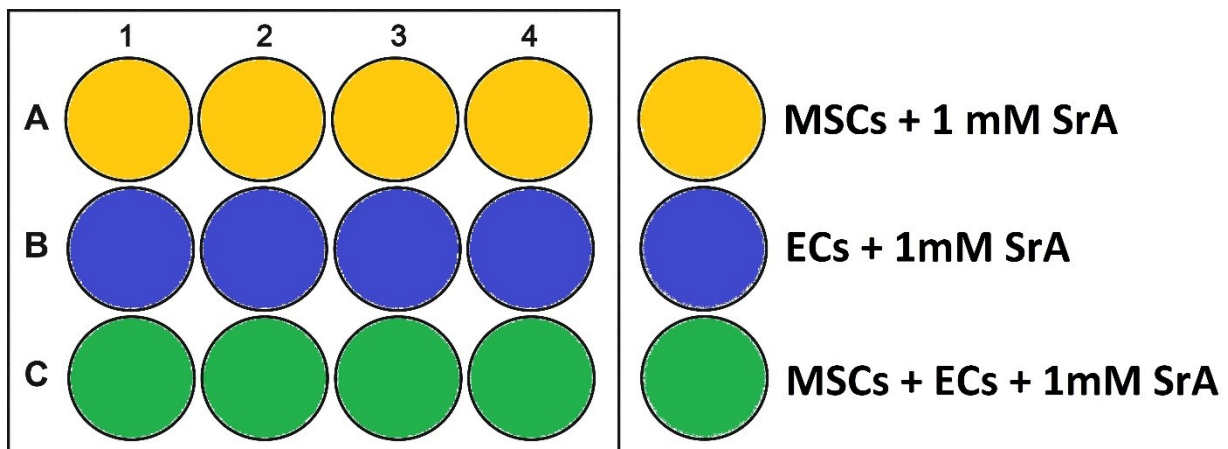


Figure 5: Layout of co-culture of MSCs and ECs - 1 mM SrA

2.5.3. Live/dead assay

The Live/Dead assay is a two-component staining that stains live and dead cells with fluorescent markers. This staining is a way to assess cell viability. Hoechst 33342, the first component, is a nucleic acid stain that binds to double stranded (ds) DNA, and will thus localise in the cell nucleus and emit blue fluorescent light [23]. The stain is excited at 346 nm and emitted at 460 nm.

Propidium Iodine (PI), the second component, is a fluorescent stain that binds to dsDNA by intercalating between nucleotides. While bound, PI emits a red fluorescent light, between 535 and 617 nm. Unlike Hoechst, PI is only permeable to dead cells, thus it stains only dead cells [24].

In 48-wells plates, 200 μ L of staining fluid is added per well, as illustrated in **Figure 6**. This staining fluid contains 197.6 μ L culture medium, 2 μ L PI (P4864, Sigma Aldrich) and 0.4 μ L Hoechst (10 mg/mL made from bisBenzimide H 33342 trihydrochloride, 14533, Sigma Aldrich). The cells are incubated for 40 minutes. Then the plate can be inspected under a fluorescence microscope using the DAPI channel (excitation 405 nm) and the TRITC channel (excitation 561 nm) to evaluate live and dead cells, respectively. The cells were counted manually using the program ImageJ.

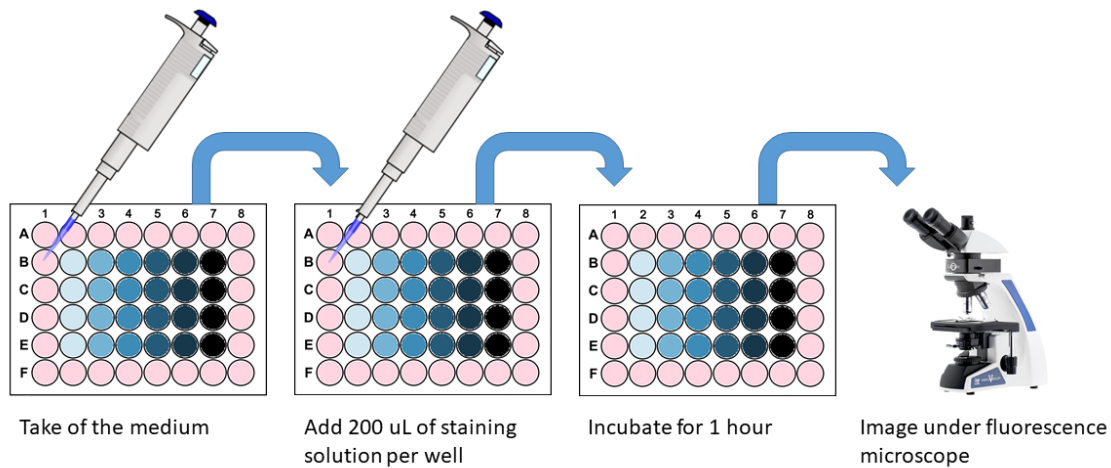


Figure 6: Live/Dead staining

2.5.4. Cell morphology characterization

The cell morphology was analyzed using SEM, as described in section 2.4.1. Implant surface characterization. To prepare MSCs on implants for SEM, implants with MSCs in culture were fixed in 1.5 mL eppendorfs using 200 μ L fixative consisting of 4% paraformaldehyde, 1% glutaraldehyde in PBS at pH 7.5. The fixative was left on the implants for at least 24 hours. Afterwards, the fixative was taken off and the implants were immersed in miliQ twice for 5 minutes, then immersed in 50% ethanol for 15 minutes, immersed in 70% ethanol for 15 minutes and finally in 96% ethanol for 20 minutes. The implants were then air-dried for 2 hours. To prepare the implants further for SEM, they needed to be electrically conductive. To achieve conductivity, the implants were cut in half and then half an implant was put on a piece of double-sided carbon tape on a metal cylinder and put in the middle of the gold sputtering machine. The implants were gold sputtered for 18 seconds.

2.5.5. Cell viability and proliferation assay

The Presto Blue assay is a way to assess metabolic activity in a cell culture. Presto Blue contains the blue dye resazurin, a component that is irreversibly reduced to resorufin by the metabolic activity of cells. Resazurin is weakly fluorescent, while resorufin is much stronger fluorescent. This can be measured through absorbance changes at 570 and 600 nm [25].

The Presto Blue assay was done by adding 20 μ L Presto Blue per well in a 48-wells plate on top of the medium (10% Presto Blue). This was also added to a few wells with only culture medium, which functioned as blanks. After adding the Presto Blue, the plate was incubated for 1 hour at 37°C, after which the absorbance was measured in a Wallac plate reader (Victor X4, Pelkin Elmer, USA) at 530 nm excitation, 570 nm emission. This procedure is also illustrated in **Figure 7**. The raw data from the samples was finally corrected for the blanks.

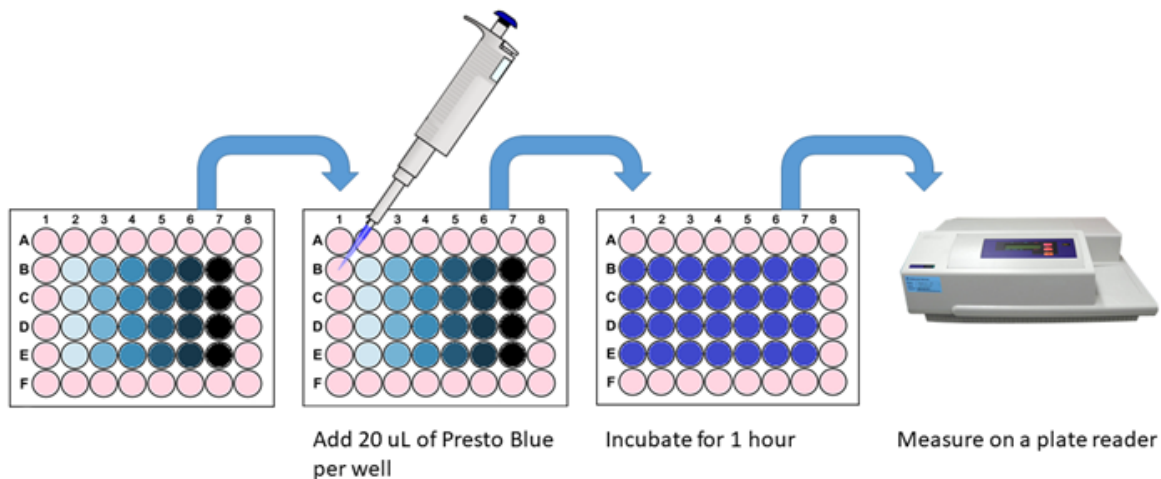


Figure 7: Schematic representation of most important steps in the Presto Blue assay procedure: Presto Blue is added, the plate is incubated for 1 hour and is then measured on a plate reader at 590 nm emission.

2.5.6. Alkaline phosphate assay

Alkaline Phosphatase is an enzyme that is an early osteogenic differentiation marker of MSCs. The activity of this enzyme can be detected using the Alkaline Phosphatase assay, wherein paranitrophenylphosphate (pNPP) is hydrolyzed into para-nitrophenol (PNP) and a phosphate. PNP is a yellow substance, with a peak absorbance at 405 nm.

ALP was measured in cellular extracts, for which the cells in culture were lysed in PBS/Triton (8% NaCl, 0.2% KCl, 1.44% Na₂HPO₄, 0.24% KH₂PO₄ and 0.1% triton in H₂O) and frozen at -80°C prior to use in the assay. Cellular extracts of MSCs on a 12-wells plate were created by putting the plate on ice, removing the medium, washing with PBS and adding 250 µL PBS/Triton to each well. The wells were then scraped thoroughly for 30 seconds, after which the cell samples were collected. The wells were then each rinsed with another 250 µL PBS/Triton, which was added to the previously collected sample. These samples were stored at -80°C until further use.

Cellular extracts of MSCs on implants were created by taking the implants out of the culture medium on days 5, 7, 14 or 21, putting them into Eppendorf tubes in PBS/triton and storing them at -80°C. For MSC cultures in 48-wells plates (excluding implants), the MSCs were directly tested in the plate on days 5, 6, 14 or 21.

For ALP measurements in MSC samples from plates, the cell extract were thawed on ice and then sonicated to fragment the cell remainders, so that all ALP was in solution and no interference of larger cell remnants could take place. The cell extracts were sonicated for 10 seconds on position 10 (Soniprep 150, MSE, Heathfield, Great Britain), or 15 seconds on position 15, when there is a lot of matrix and calcium in the samples so optimal fragmentation of the cell remnants could be achieved.

For ALP measurements in MSCs that were cultured on implants, the samples in the Eppendorf tubes were thawed on ice and then sonicated using a sonication water bath for 5 minutes.

While the samples in the Eppendorf tubes are being thawed, a set of PNP (1M PNP in dietholamine buffer) standards, as in **Table 3**, were made in 5 mL PS tubes *in duplo*. Then 100 μL PBS/triton and 250 μL NaOH (0.1M NaOH in H_2O) are added to the standards.

Table 3: set of PNP standards

μL PNP	μL dietholamine buffer	mM PNP
0	100	0.00
5	95	0.05
10	90	0.10
15	85	0.15
20	80	0.20
30	70	0.30
40	60	0.40
50	50	0.50
75	25	0.75
100	0	1.00

These standards provide a means to convert the measured samples to a PNP conversion rate. First, 100 μL of the samples were pipetted *in duplo* in 5 mL PS tubes. Per tube, 100 μL PNPP (20 mM PNPP in dietholamine buffer) was added. The tube was vortexed and incubated at 37°C in a waterbath. After 10 seconds, 100 μL PNPP was added to the second tube, vortexed and incubated and so on. Each tube was kept in the waterbath for exactly 10 minutes, after which the reaction was stopped with 200 μL NaOH and the tube was placed on ice. Of each standard and sample, 200 μL was pipetted into a microplate (96-wells) and the absorbance was measured at 405 nm on a plate reader (Victor X4, Perkin Elmer, Waltham, USA).

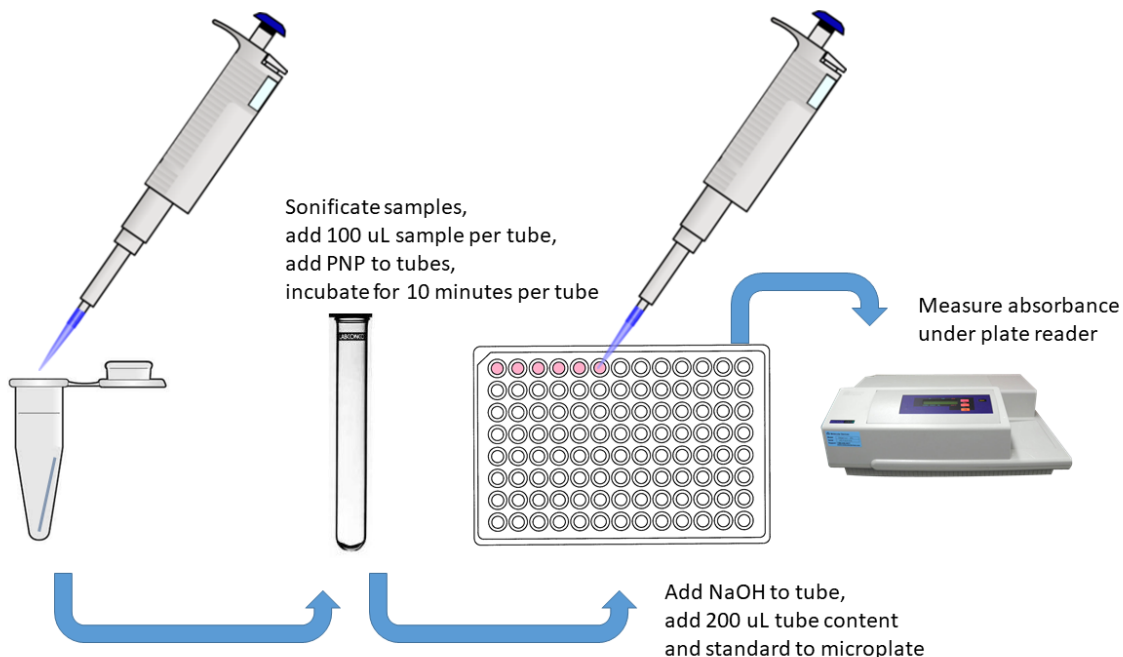


Figure 8: Schematic representation of most important steps in the ALP assay procedure

2.5.7. BCA assay

The Pierce BCA protein Assay (Thermo Fischer) was used to measure protein. It contains reagent A (sodium carbonate, bicinchonic acid and sodium tartrate in 0.1 M sodium hydroxide), reagent B (4% cupric sulfate) and Albumin (2.0 mg/mL in PBS/Triton). First, the samples were thawed on ice. While thawing, the standards in **Table 4** were made *in duplo* in 1.5 mL Eppendorf tubes.

Table 4: BSA standard

Tube	Volume of diluent (PBS/triton)	Volume and source of BSA	Final BSA concentration
A	300 μ L	100 μ L of stock	500 μ g/mL
B	200 μ L	200 μ L of A dilution	250 μ g/mL
C	250 μ L	250 μ L of B dilution	125 μ g/mL
D	150 μ L	300 μ L of C dilution	83.3 μ g/mL
E	200 μ L	200 μ L of D dilution	41.7 μ g/mL
F	200 μ L	200 μ L of E dilution	20.8 μ g/mL
G	150 μ L	0 μ L	0 μ g/mL

BCA working reagent was prepared by mixing 50 parts of BCA reagent A with 1 part of BCA reagent B (50:1). 200 μ L of working reagent was needed for each sample. The working reagent is stable for one day at room temperature in a closed container.

Of the thawed samples, 25 μ L of each sample was pipetted into a 96 wells plate in duplo. Then 200 μ L of working reagent was added to each sample. The plate was covered and incubated at 37°C for 30

minutes. The absorbance was then measured at 595 nm on a plate reader. The protein content was calculated using the standard and was then corrected for sample volume, and additionally plate surface, if the cells were cultured on a plate (excluding MSCs on implants).

2.5.8. qRT-PCR

Quantitative real-time polymerase chain reaction (qRT-PCR) is a way to measure (relative) gene expression. To prepare samples for qRT-PCR, a plate with live cells was kept on ice, while the medium was taken off. The cells were washed twice with PBS, after which trizol was added (500 μ L per well in a 12-wells plate). The wells were then scraped and the lysate was stored at -20°C . After freezing, the lysates were thawed on ice and 100 μ L of chloroform was added to each sample. The samples were then gently rocked 15 times and stored on ice for 10 minutes. Then the samples were centrifuged at 4°C at $14.000\times g$ for 20 minutes. Finally, 300 μ L isopropanol was added to each sample and they were rocked a few times after which they were stored overnight. One day later, the samples were centrifuged at 4°C at $14.000\times g$ for 40 minutes. The supernatant was then taken off by slowly tilting the eppendorf containing the sample into the vacuum tip. The pellets were washed 3 X with 70% ethanol and centrifuged for maximum 2 minutes in between. The pellets were then washed with 100% ethanol and centrifuged. The ethanol was then taken off and the pellets were air dried upside down for max 5 minutes. Finally, 12 μ L nuclease-free water was added to each sample and mixed and they were stored at -80°C .

For cDNA synthesis, the samples were thawed and the amount of RNA in each sample was measured using a spectrophotometer (Denovix, Wilmington, USA). Then the samples were diluted to reach the same final concentration of 40.0385 $\mu\text{g}/\mu\text{L}$ RNA in all of them. To each sample, 1 μL oligo dT and 1 μL hexamer primers was added. The samples were spun down shortly afterwards and then heated at 70°C for 5 minutes. Then a mix of 4 μL buffer, 2 μL dNTP, 1 μL RNase inhibitor and 1 μL Taq polymerase enzyme was added to each sample, except for the $-RT$ (reverse transcriptase): 1 μL nuclease-free water was added instead of the enzyme to function as a negative control (no cDNA will be generated). The samples were spun down shortly and then heated for 60 minutes at 42°C and subsequently heated for 10 minutes at 70°C . Finally, 230 μL of nuclease-free sample was added to each sample and they were stored at -20°C .

For the qRT-PCR, the samples were thawed and the new forward and reverse primer vascular endothelial growth factor A-1 (VEGFA1), Mucin 1 (MUC1) and Hypoxia-inducible factor 1-alpha (HIF1A) as well as the housekeeping gene GAPDH were dissolved to 250 pmol/ μL stocks and then 50 X diluted to 5 pmol/ μL work stocks. The sequences for these primers can be found in section 8.5 Primer sequences for PCR. The primers from work stock were used to make a mix for each gene, as shown in **Table 5**. In a PCR plate, 2 μL of cDNA was added and then 23 μL of primer mix was added to each sample. The plate was placed into the PCR machine. The PCR machine ran in three steps and then had a melting curve step. The first step ran for 2 minutes at 50°C , after which the second step lasted for 10 minutes at 95°C . Then the third step consisted of 40 repetitions of 15 seconds at 95°C and then 1 minute at 60°C . The fourth and final step consisted of alternating 15 seconds at 95°C and then 1 minute at 60°C until the sample volume completely evaporated. The gene expression was corrected for GAPDH expression.

Table 5: Primermix for qRTPCR

Ingredient	GAPDH, HIF1A	VEGFA1, MUC1
Mastermix	12.5	12.5
Forward primer	0.5	1
Reverse primer	0.5	1
Nuclease-free water	9.5	8.5

2.6 Statistics

All the results shown are presented as mean value \pm standard deviation of the mean. The results of all the experiments were analyzed with Kruskal-Wallis tests and subsequent Mann-Whitney tests comparing individual conditions using the Graphpad Prism 5.03 software. The results were deemed significant with p-value lower than 0.05.

3. Results

3.1 Biomaterial synthesis

3.1.1. Voltage-time response of plasma electrolytic oxidation treatment

The voltage transient (V-t) was recorded during the PEO process and is shown in **Figure 9**. After initiating the process, the voltage rose sharply for about 7 seconds, after which dielectric breakdown took place. Dielectric breakdown formed the transition point from a highly increasing voltage rate to a slowly increasing voltage rate. From this stage onwards, homogeneously distributed plasma discharges along the surface of the implant were initiated and could be observed as sparking along the implant. After dielectric breakdown, the rise in voltage slowed down until the end of the PEO process.

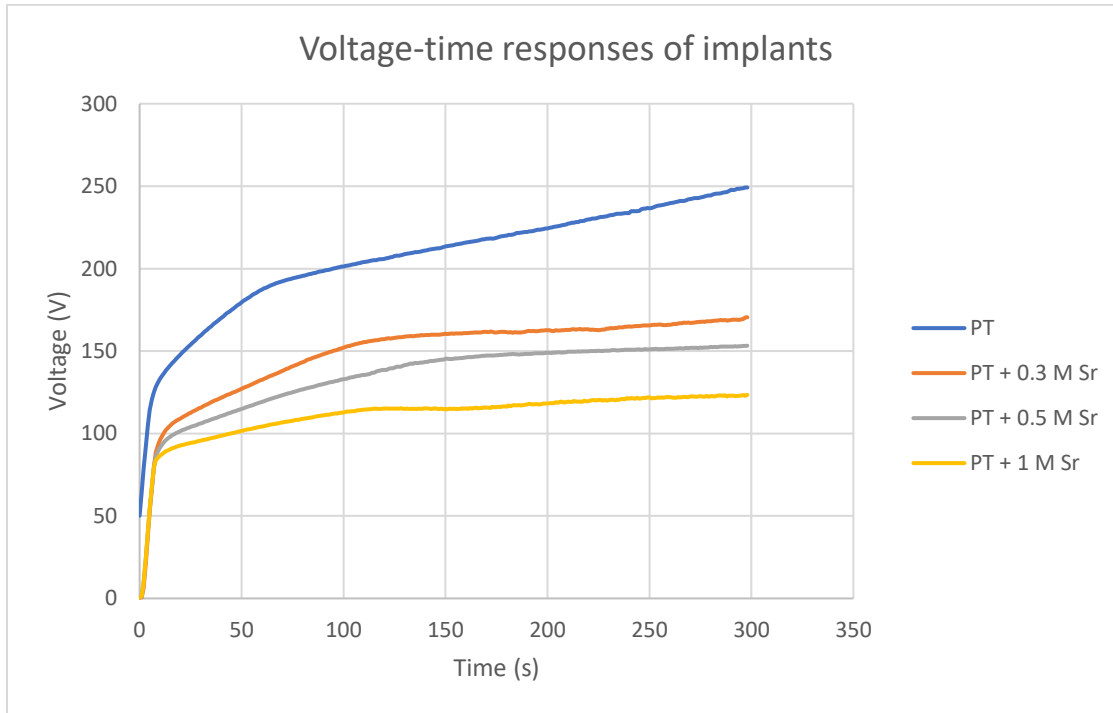


Figure 9: The voltage-time response of implants, PT = PEO treated

The recorded voltage responses of the implants showed a higher initial increase rate in the PT + Sr groups than in the PT group (**Table 6**). The voltage of PT also rose more than the PT + Sr groups, whose voltages rose slower with increasing strontium concentration in the electrolyte. After 300 seconds the final voltages had a similar trend: highest in PT and then decreasing with increasing strontium concentration in the electrolyte.

Table 6: Average increasing rates and final value of voltages for each type of PEO treated implant, N=10

Type of implant	Initial increase rate of voltage (V/s)	Average increase rate of voltage after dielectric breakdown (V/s)	Final voltage (V)
PT	14.0±1.0	0.49	249.2±6.0
PT + 0.3 M Sr	11.3±1.5	0.28	170.7±3.6
PT + 0.5 M Sr	11.3±0.8	0.23	153.2±1.9
PT + 1 M Sr	11.3±2.2	0.15	123.3±1.1

3.2. Biomaterial Characterization

3.2.1 Surface morphology of implants after plasma electrolytic oxidation treatment

The surface morphology of the implants after PEO treatment was analyzed by SEM (**Figure 10**). SEM examination of the surface morphologies of the implants showed the homogenous coverage of the implants with a porous TiO_2 layer. With increasing amounts of strontium in the electrolyte, the size of the pores decreases. This is especially visible in the PT + 1 M Sr condition.

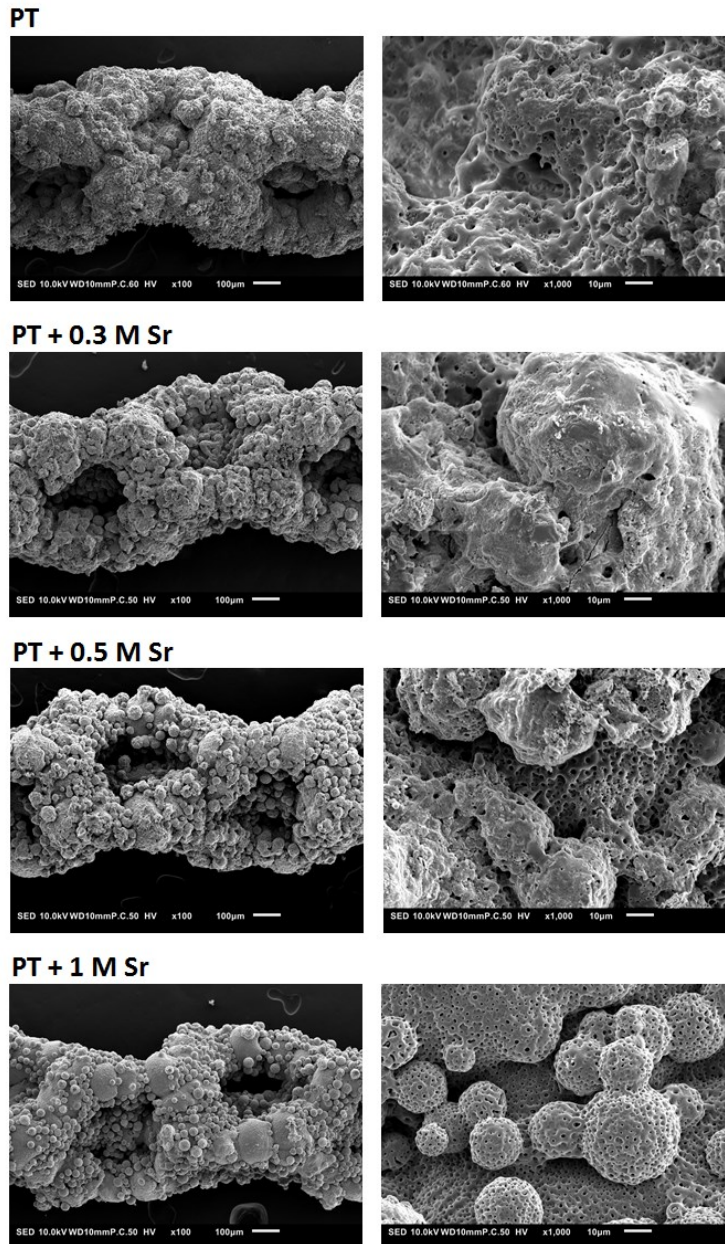


Figure 10: Surface morphology of PT, PT + 0.3 M Sr, PT + 0.5 M Sr and PT + 1 M Sr implants after PEO treatment as revealed by SEM in x100 and x1000 magnification.

3.2.1 Ion release profile of implants

The Sr ion release was measured by ICP-OES and is shown in **Figure 11** in mass parts per billion (ppb). The highest Sr²⁺ ion release came from the PT + 0.3 M Sr group, then from the PT + 0.5 M group and the lowest release from the PT + 1 M Sr group. The release converted to mM is shown in section 8.4 Release of strontium in molar of the Appendix.

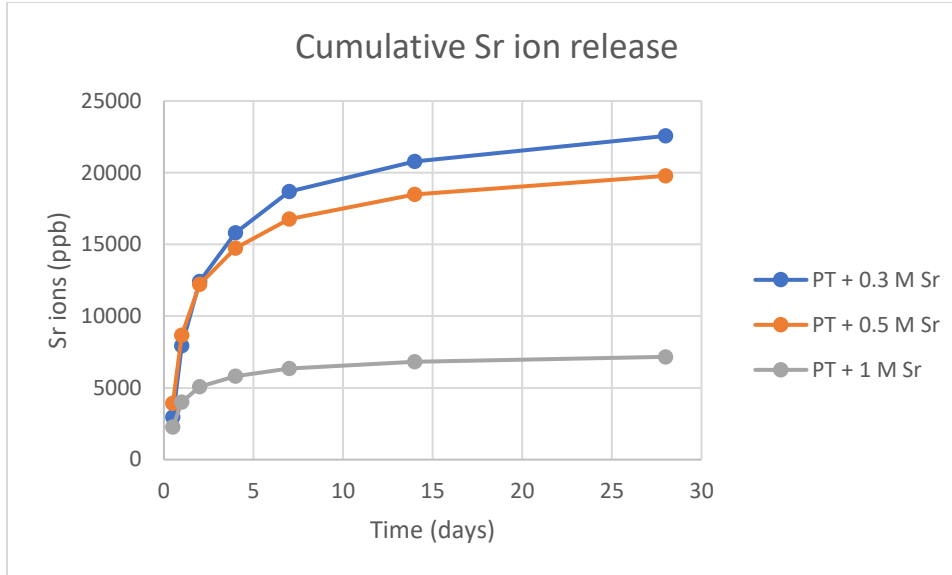


Figure 11: Cumulative Sr ion release profile for the implant groups (n=3) in parts per billion

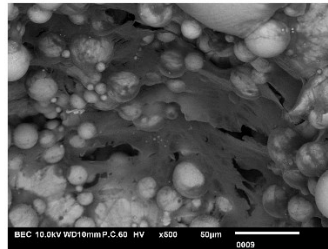
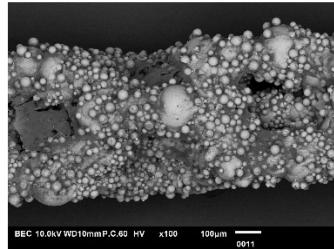
3.3. In-vitro tests

3.3.1 In-vitro experiments on MSCs implants

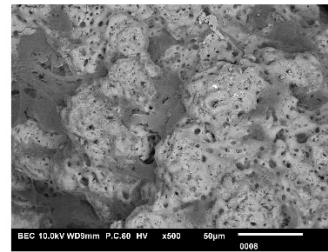
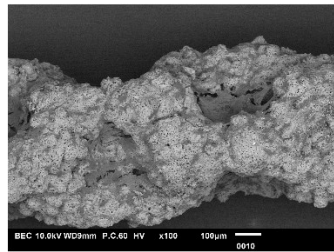
3.3.1.1. Cell morphology of MSCs on implants

The cell morphology and extent of coverage on the different types of implants was evaluated by SEM on the day of seeding (d-2), day of differentiation (d0), day 3, day 5, and day 14. The results from day -2, day 3 and day 5 can be found in the appendix (“8.3 SEM images of MSCs on implants”). In every condition, cells attached to the surface of the implant, however the extent of coverage and morphology was different between conditions. **Figure 12** shows MSCs with a 2 hour seeding time on the different types of implants after 14 days of culture. On day 14, the MSCs covered a large part of the implants. The coverage of the NT, PT + 0.3 M Sr and PT + 0.5 M Sr had a similar extent of coverage. There was less coverage of the PT and PT + 1 M Sr implants. Furthermore, the morphology of all the PEO-treated implants was similar: the MSCs were stretched out over large parts of the implant. In contrast, on the NT implant, cells stretch over smaller areas and had a rounder shape. This is especially visible in **Figure 13**, which compares the morphology of 1 hour vs 2 hours seeding time of MSCs on implants on day 0. This figure shows an increased amount of cells on the PT + 0.3 M Sr and PT + 0.5 M Sr implants. Additionally, more cells are present on the implants of the 2 hours vs 1 hour seeding group.

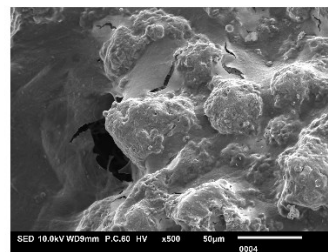
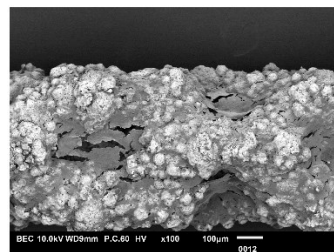
NT



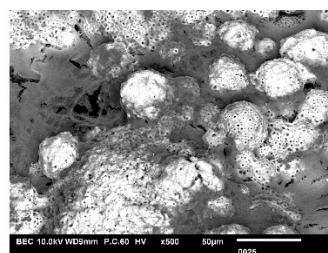
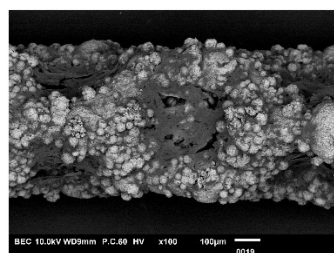
PT



PT + 0.3 M Sr



PT + 0.5 M Sr



PT + 1 M Sr

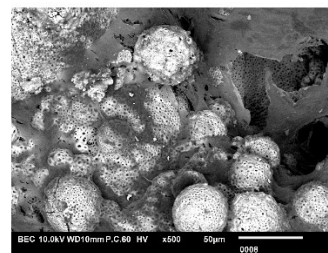
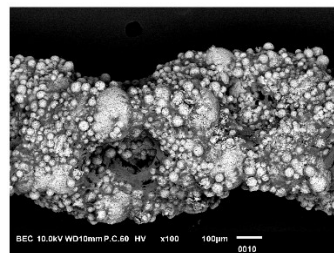


Figure 12: SEM images of cell morphology and spreading of MSCs on implants with 2 hour seeding time (left) and on day 14 (right), 100x and 500x magnification

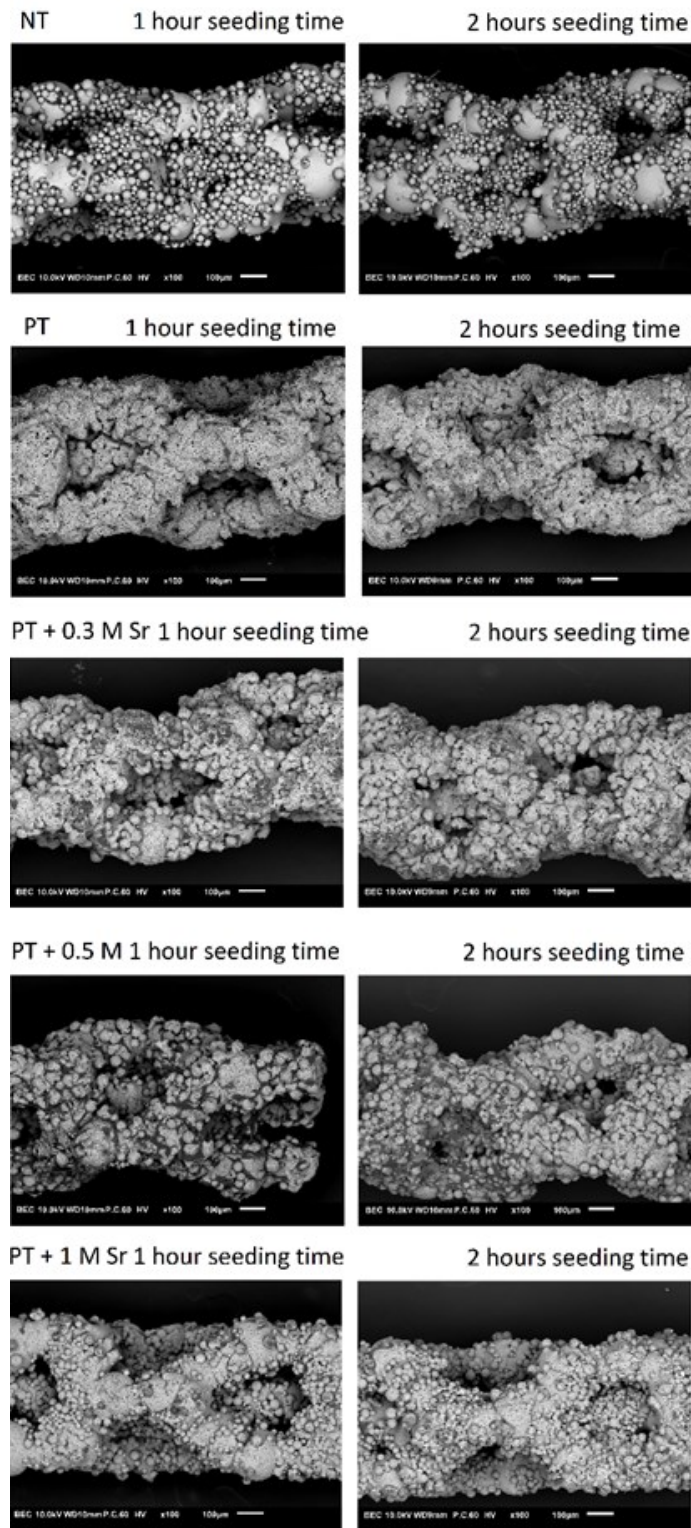


Figure 13: SEM images of cell morphology and spreading of MSCs on implants with 1 hour and 2 hours seeding time, on day 0, 100x magnification

3.3.1.2. Viability of MSCs on implants

The viability of MSCs on implants was evaluated by a custom Live/Dead assay on day 0 of culturing on implants. The trend, as shown in **Table 7**, clearly demonstrates a lower viability of MSCs on NT implants and slightly lower viability on PT implants, compared to strontium incorporated conditions. The strontium incorporated implants had a similar viability. The total amount of cells on the implants differs per implant type: NT and PT + 1 M Sr implants have most cells attached to it, although most of the cells on the NT implants were dead. The amount of cells on PT, PT + 0.3 M Sr and PT + 0.5 M Sr implants were similar to each other.

Table 7: Viability of MSCs on implants on day 0, N = 2, 2 hour seeding time

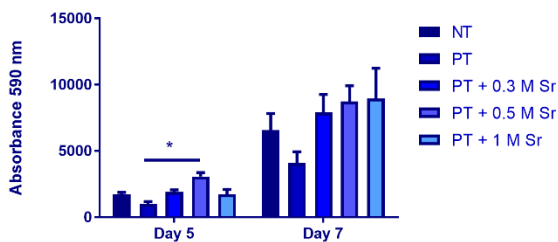
Type of implant	Live Cells	Dead cells	Total cells	Viability (%)
NT	281.5 ± 137.9	302 ± 141.4	583.5 ± 3.5	48.3 ± 23.9
PT	179.5 ± 20.56	91 ± 84.9	270.5 ± 64.3	69.2 ± 24
PT + 0.3 M Sr	183 ± 28.3	25 ± 4.2	208 ± 24	87.8 ± 3.5
PT + 0.5 M Sr	233.5 ± 20.5	32 ± 5.7	255.5 ± 14.8	87.4 ± 2.9
PT + 1 M Sr	369 ± 66.4	70.5 ± 31.8	439.5 ± 34.6	83.6 ± 8.5

3.3.1.3. Metabolic activity of MSCs on implants

The metabolic activity of MSCs on implants was assessed using the Presto Blue assay. **Figure 14A** shows the metabolic activity of MSCs on implants with 1 hour seeding time on day 5 and day 7; **Figure 14B** shows the metabolic activity of MSCs on implants with 2 hour seeding time on day 3, day 5, day 7, day 10 and day 14. The 1 and 2 hours seeding time showed big differences. In the 1 hour seeding time condition, the trend in the metabolic activity shows an increasing activity with increasing strontium condition and a higher activity of MSCs on NT implants than on PT implants. The effect is significant between PT compared to PT + 0.5 M Sr ($p = 0.0109$) on day 5. On day 7, no significant effects were found. The trend in the 1 hour condition is shown on day 7 in the 2 hour conditions. A significant difference was observed between NT compared to PT + 1 M Sr ($p = 0.01$), PT compared to PT + 0.3 M Sr ($p = 0.0375$), PT compared to PT + 0.5 M Sr ($p = 0.0345$) and PT compared to PT + 1 M Sr ($p < 0.001$) on day 7. However, all the other time points show a different trend. Day 3 and day 5, which were done on the same plate, show a trend where the metabolic activity, from high to low, $PT \approx PT + 1 \text{ M Sr} > PT + 0.3 \text{ M Sr} > PT + 0.5 \text{ M Sr}$. The differences were not significant. On day 10 and 14, which were also measured on the same plate, the trend in the metabolic activity from high to low shows $NT \approx PT + 0.5 \text{ M Sr} > PT \approx PT + 1 \text{ M Sr} > PT + 0.3 \text{ M Sr}$. There were also no significant differences between any of the conditions on these time points.

A

Presto Blue of MSCs on implants - 1 hour seeding time

**B**

Presto Blue of MSCs on implants - 2 hours seeding time

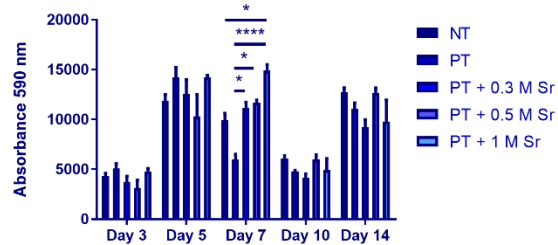


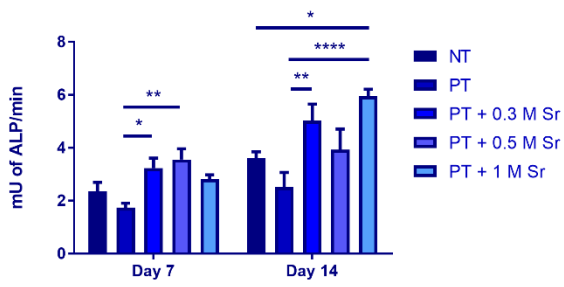
Figure 14: Presto Blue of MSCs on implants. A: 1 hour seeding time on day 5 and 7, B: 2 hour seeding time on various time points
 * = $p < 0.05$, ** = $p < 0.01$, *** = $p < 0.001$, **** = $p < 0.0001$

3.3.1.4. Differentiation of MSCs on implants

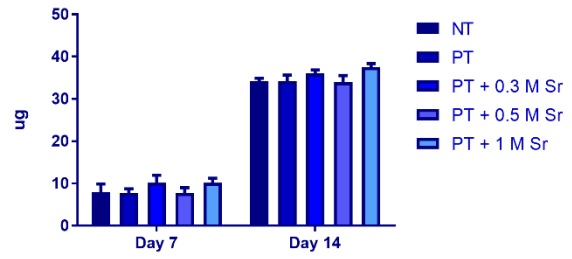
The extent of (early) differentiation of MSCs on implants was assessed using an ALP and BCA assay: the ALP assay to measure the extent of starting differentiation and the BCA to correct for the relative number of cells. While using 1 hour seeding time (**Figure 15**), ALP generally goes up with increasing strontium concentration in the electrolyte (excluding PT + 1 M Sr on day 7 and PT + 0.5 M Sr on day 14). This is shown by a significant difference between NT compared to PT + 1 M Sr ($p = 0.0121$), PT compared to PT + 0.3 M Sr ($p = 0.0062$) and PT compared to PT + 1 M Sr ($p < 0.0001$) on day 14. Due to the amount of cells, the ALP production corrected for the amount of cells shows the highest ALP activity in the NT and PT + 0.5 M Sr group, followed by the PT + 1 M Sr and PT + 0.3 M Sr groups. However, the only significant difference was between PT compared to PT + 0.5 M Sr ($p = 0.0073$) on day 7. There was no significant difference between any of the 1 hour seeding time conditions in BCA. In the 2 hour seeding time groups (**Figure 16**), the effects were different: the ALP and BCA trends generally show increased ALP with increased strontium concentrations in the electrolyte. This was shown by a significant difference between PT compared to PT + 0.5 M Sr ($p = 0.0344$) on day 14. Furthermore, the ALP activity showed significant increase after PEO treatment, as shown by the significant differences between NT compared to PT ($p = 0.0160$), NT compared to PT + 0.5 M Sr ($p = 0.0041$) and NT compared to PT + 1 M Sr ($p = 0.0011$) on day 11 and by NT compared to PT + 0.5 M Sr ($p = 0.0439$) on day 14. The protein also increased with increasing strontium in the electrolyte (except 0.3 M Sr on day 11), with significant differences between PT compared to PT + 1 M Sr ($p = 0.0242$) and PT + 0.3 M Sr compared to PT + 1 M Sr ($p = 0.0071$) on day 11. After correction for protein, the corrected ALP activity decreases with increasing concentration of strontium in the electrolyte, due to a higher increase in BCA than in ALP with increasing strontium. Due to relative high BCA on NT implants on day 11 and day 14, the ALP corrected for protein is much smaller compared to the other conditions. These findings are shown by significant differences on day 11 between NT compared to PT ($p = 0.0009$), NT compared to PT + 0.3 M Sr ($p = 0.0034$) and PT compared to PT + 1 M Sr ($p = 0.0372$). On day 14, they are shown by a significant difference between NT compared to PT + 0.5 M Sr ($p = 0.0405$).

A

ALP of MSCs on implants - 1 hour seeding time

**B**

BCA of MSCs on implants - 1 hour seeding time

**C**

ALP corrected for protein of MSCs on implants - 1 hour seeding time

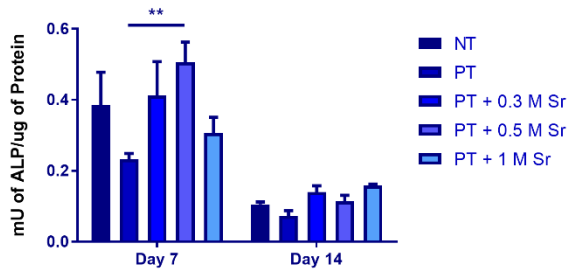
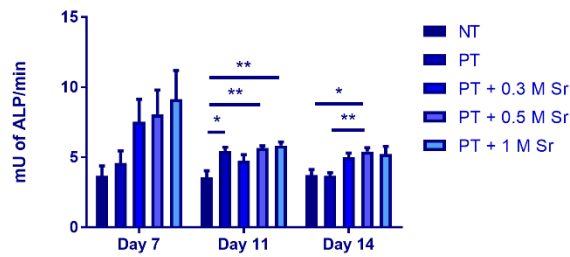


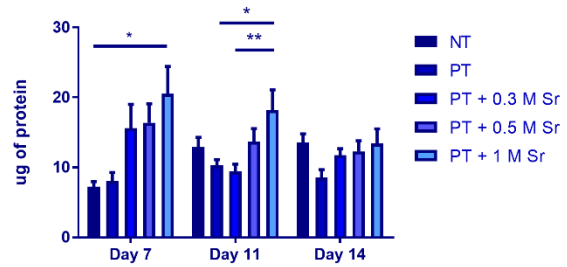
Figure 15: A: ALP of MSCs on implants with 1 hour seeding time on various time points, B: BCA of MSCs on implants with 1 hour seeding time on various time points, C: ALP corrected for protein of MSCs on implants with 1 hour seeding time on various time points, * = $p < 0.05$, ** = $P < 0.01$, *** = $p < 0.001$

A

ALP of MSCs on implants - 2 hours seeding time

**B**

BCA of MSCs on implants - 2 hours seeding time

**C**

ALP corrected for protein of MSCs on implants - 2 hours seeding time

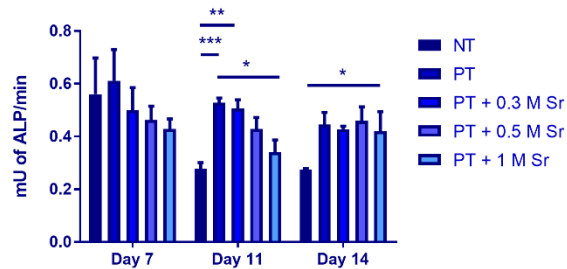


Figure 16: A: ALP of MSCs on implants with 2 hour seeding time on various time points, B: BCA of MSCs on implants with 2 hour seeding time on various time points, C: ALP corrected for protein of MSCs on implants with 2 hour seeding time on various time points, * = $p < 0.05$, ** = $P < 0.01$, *** = $p < 0.001$

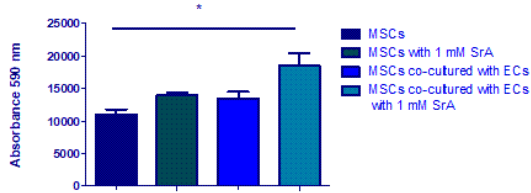
3.3.2. Co-cultures of MSCs and ECs with strontium

3.3.2.1. Metabolic activity of MSCs and ECs in co-culture with strontium

The metabolic activity was measured by a Presto Blue assay. MSCs and ECs were separated before the assay was performed by moving the transwells to a different plate. Subsequently, a Presto Blue assay was done. The metabolic activity of ECs and MSCs are shown in **Figure 17**. The MSCs differed significantly between the MSCs and MSCs in co-culture with ECs with 1 mM SrA condition ($p = 0.046$) (**Figure 17A**), but no significant difference was found between the metabolic activity in ECs (**Figure 17B**).

A

Presto Blue of MSCs in co-culture with ECs and with 1 mM SrA

**B**

Presto Blue of ECs in co-culture with MSCs with 1 mM SrA

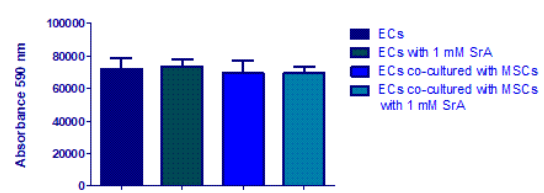


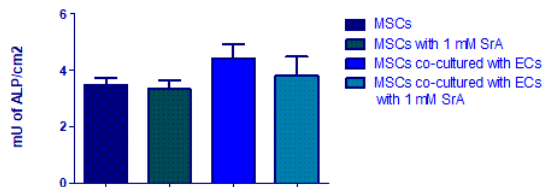
Figure 17: A: Presto Blue of ECs in co-culture with MSCs and/or 1 mM SrA on day 2, B: Presto Blue of MSCs in co-culture with ECs and/or 1 mM SrA on day 2, * = $p < 0.05$

3.3.2.2. Differentiation of MSCs in co-culture with ECs and strontium

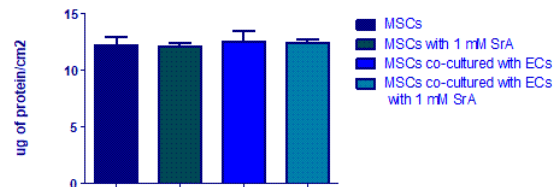
The ALP activity, protein content and ALP corrected for protein of MSCs in co-culture and with 1 mM SrA are shown in **Figure 18**. The trend in the uncorrected ALP shows a higher ALP activity in the MSC co-cultured with ECs group and this trend is confirmed in the corrected ALP activity levels, where the trend still shows. The protein content is similar between all conditions.

A

ALP of MSCs in co-culture with ECs and with 1 mM SrA

**B**

BCA of MSCs in co-culture with ECs and with 1 mM SrA

**C**

ALP corrected for protein of MSCs in co-culture with ECs with 1 mM SrA

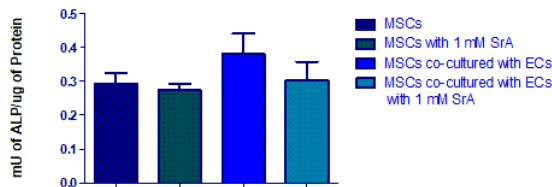


Figure 18: A: ALP of MSCs in co-culture with ECs and/or 1 mM SrA on day 6, B: BCA of MSCs in co-culture with ECs and/or 1 mM SrA on day 6, C: ALP of MSCs in co-culture with ECs and/or 1 mM SrA on day 6

3.3.2.3. Differentiation of ECs in co-culture with MSCs and strontium

To assess endothelial cell differentiation, gene expression of *HIF1A*, *MUC1* and *VEGFA1* was assessed using PCR (**Figure 19**). Co-culture with MSCs downregulates the gene expression of *VEGF-A1* in ECs, as shown by the significant differences between ECs compared to ECs co-cultured with MSCs ($p = 0.0286$) and ECs with 1 mM SrA compared to ECs co-cultured with MSCs with 1 mM SrA ($p = 0.0286$). Additionally, strontium might upregulate the expression of *VEGF-A1*, as shown by the trend between ECs and ECs with 1 mM SrA ($p = 0.0571$). No significant differences between any of the conditions were found in the gene expression of the other genes.

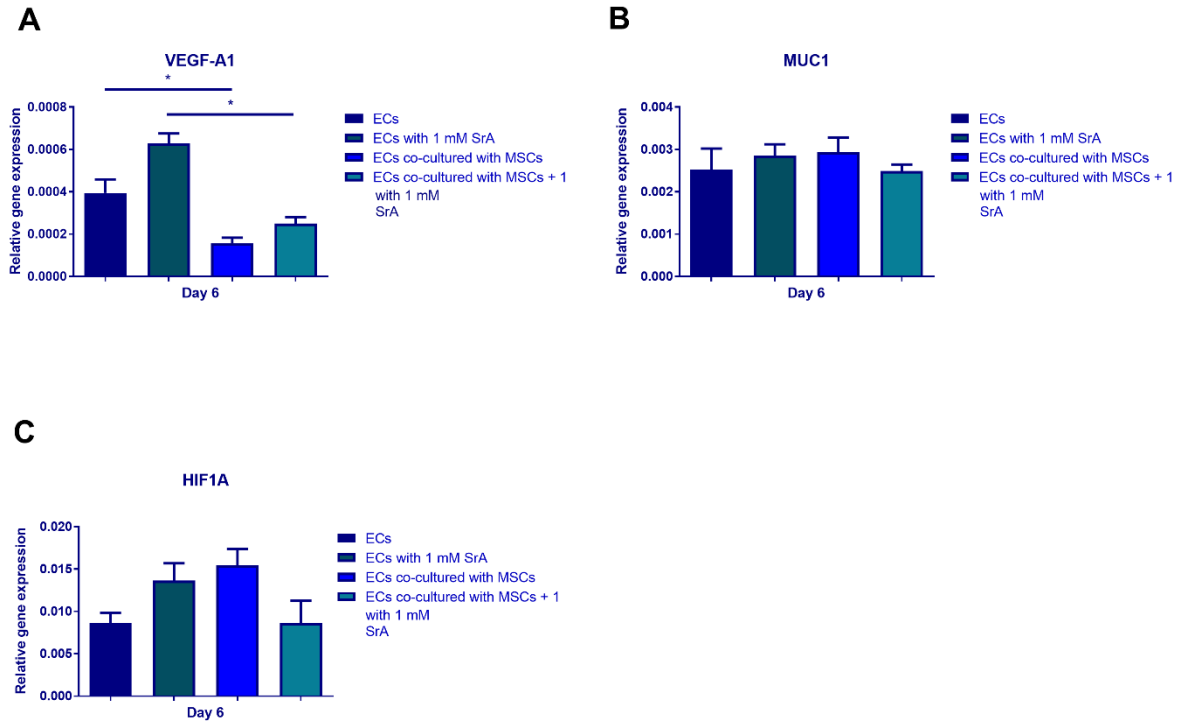


Figure 19: A: *HIF1A* expression of ECs in co-culture with MSCs and/or 1 mM SrA on day 6, B: *MUC1* expression of ECs in co-culture with MSCs and/or 1 mM SrA on day 6, C: *VEGF-A1* expression of ECs in co-culture with MSCs and/or 1 mM SrA on day 6, * = $p < 0.05$

4. Discussion

In the first part of this study, strontium-incorporated-and-releasing titanium implants were made using PEO. Subsequently, the osteogenic effects of biofunctionalized implants on MSCs were assessed. Additionally, the influence of strontium on co-cultures of MSCs and ECs and their mutual effects were assessed. The first part of this study resulted in five implants conditions: the NT, PT, PT + 0.3 M Sr, PT + 0.5 M Sr and PT + 1 M Sr conditions. In the PEO treated conditions, the voltage-time curves decreased with increasing concentration of strontium in the electrolyte. Additionally, in the morphology of the PEO treated implants the pore size decreased with increasing concentration of strontium. Subsequently, the ion release profiles showed the largest cumulative and non-cumulative Sr^{2+} release in the PT + 0.3 M Sr condition, then in the PT + 0.5 M Sr condition and finally the lowest release in the PT + 1 M Sr condition. After these measurements, the effects of the implants on morphology, viability, metabolic activity and differentiation of MSCs were assessed. Starting with the morphology of MSCs on implants, the

morphology of MSCs on the implants varied over time and condition. The morphology of the cells was most contrasting between the NT condition compared to all the PEO treated conditions. In the NT condition, cells stretched over smaller areas and had a rounder shape than in the PEO treated conditions, where the cells stretched over large parts of the implant, an indication of healthy bone precursor cells [26]. One of the most striking results was the increase in cell numbers on implants in the 2 hour seeding time condition. Additionally, most cells were found on the PT + 0.3 M Sr and PT + 0.5 M Sr implants in both the 1 hour and 2 hour conditions. Besides the morphology, the viability of the cells on the implants was studied. NT had the lowest viability, followed by PT. The strontium incorporated conditions had improved viability compared to PT and were similar to each other. The metabolic activity of the MSCs on implants, which was subsequently measured, revealed increasing metabolic activity with increasing strontium concentration in the 1 hour seeding time. However, the trends on the 2 hour seeding time were not consistent between time points and showed an increasing trend with increasing strontium concentration on day 3, day 5 and day 7, but a somewhat decreasing trend with increasing strontium on day 10 and day 14. As a final test, the differentiation of MSCs on implants was assessed by measuring ALP activity and protein content. In both the 1 and 2 hour seeding time conditions, the ALP activity generally increased with increasing strontium concentration, but the protein contents were different. In the 1 hour seeding time condition, no differences were found between conditions, while in the 2 hour condition, protein content increased with strontium concentration. This caused a difference in the ALP activity corrected for protein, where, in the 1 hour seeding time condition, the ALP activity still increased with increasing strontium concentration, but in the 2 hour seeding time condition, the ALP decreased with increasing strontium concentration due to the larger increase in protein.

Continuing on to the co-cultures, the first assessed parameter on the co-cultures was a Presto Blue assay, which determined the metabolic activity of the cells. There were only significant differences between MSCs compared to MSCs in co-culture with ECs with 1 mM SrA condition, indicating an effect of both strontium and co-culture. After the metabolic activity, the differentiation of both MSCs and ECs were assessed using ALP and BCA assays and a PCR, respectively. The trend in the uncorrected ALP showed a higher ALP activity in the MSC co-cultured with ECs condition compared to the MSCs condition and this trend was confirmed in the corrected ALP activity levels, where the trend still showed. The protein content was similar between all conditions. The PCR however, showed that the gene expression of *VEGF-A1* in ECs was downregulated by co-culture with MSCs. A trend showed upregulation of *VEGF-A1* as a result of adding strontium. VEGF-A is an early marker of angiogenesis and is known to induce angiogenesis in ECs [27]. MUC1 lies further downstream of VEGF-A, and plays a role in hypoxia driven angiogenesis [28]. HIF1A also plays a role in this type of angiogenesis [29, 30].

4.1 Implant characteristics resulting from the PEO process

The strontium release profile as shown in **Figure 11** displays lower Sr²⁺ release in the implants with higher strontium concentrations in the electrolyte. A possible explanation for this unexpected result is the poorer conductance of electrolytes with a larger concentration of charged particles [31]. Poorer conductance could cause a reduced growth rate of the oxide layer leading to less incorporation of strontium. There are only a small amount of papers that research the effects of PEO incorporated strontium on titanium implants and even less studies measure the actual Sr²⁺ release. The present study also included more strontium than ever before and is also the only one that both measured Sr²⁺ release and tested multiple strontium concentrations in the electrolyte. Earlier studies found similar patterns of ion release, although in a much lower range due to low strontium concentrations in the electrolytes

used [32-34]. The use of additional particles in the electrolyte caused a lower Sr^{2+} release, presumably due to less incorporation of strontium due to poorer conductance of the electrolyte [34]. The results in this study thus are in line with existing literature. The morphology of the implants with increasing strontium concentrations in the electrolyte confirms the theory of poorer conductance by showing a different morphology: smaller pores with increasing strontium concentration in the electrolyte. The smaller pores could suggest a lowered oxidation rate, resulting in smaller pores. Smaller pores have been found before in strontium incorporated PEO treated titanium implants, especially with increasing concentration of strontium [35-38]. The lower average increase rate of voltage after dielectric breakdown and lower final voltage with increasing strontium concentration in the electrolyte from the V-t curves suggest a less efficient PEO process with increasing strontium concentration. This could be caused by the poorer conductance in those electrolytes. Literature confirms this by showing a lower dielectric breakdown, initial increase rate of voltage, average increase rate of voltage after dielectric breakdown, and final voltage as a result of an increasing concentration of particles in the electrolyte [39]. Another striking result regarding the strontium release profile is the fast decrease in release over time. This pattern was confirmed to be typical by earlier literature [32-34]. The effective range of strontium in medium added to MSCs was determined to be around 1 mM SrA (see section 8.1 Effects of Strontium in medium). In earlier literature, the effective range was determined to be between 0.01–0.10 mM on MSCs [40]. The PT + 0.3 and PT + 0.5 M implants show an initial release that approaches to 1 mM SrA, but the release drops thereafter in a way that the effect of strontium ions on MSCs at a later time point may not be effective. Strontium release probably influences the MSCs initially during attachment and early differentiation but after the first refreshment of the cells, there will hardly be any strontium ions released into the medium. However, this is similar in earlier results, where the strontium dose also decreases rapidly [32-34]. In earlier studies where the strontium concentration was comparable, the results concerning differentiation were similar compared to PT + 0.3 M Sr and PT + 0.5 M Sr, although they were performed in rat MSCs [32]. Metabolic activity of bone cells as a result of this strontium release has not been measured before. The metabolic activity, ALP and BCA could have been the result of the initial (burst of) strontium release, but it is also possible that the changed morphology had this effect. However, the visible differences in morphology of the PT compared to the PT + 0.3 M Sr and PT compared to the PT + 0.5 M Sr were slim. In these conditions, the pore size is probably not a variable of influence. However, the thickness of the oxide layer is probably decreased with increasing strontium concentration due to the lower V-t curves that were discussed previously. The thickness of the oxide layers could have affected the MSCs.

4.2 1 hour vs 2 hours seeding time

The seeding time appeared to have an important influence on the way strontium affected MSCs. Initially, 1 hour seeding time was used, but this resulted in only a small amount of usable sample. The 2 hours seeding time was therefore used to optimize the protocol, since it was hypothesized to only increase the amount of usable sample. The amount of usable sample increased, but the conditions also differed from each other while this was not expected. Compared to 1 hour, 2 hours seeding time increased the amount of cells attaching to the implants and improved the detection of ALP activity, as more cells were present on the implants. These were expected differences as more cells were hypothesized to attach to the implants in 2 hours compared to 1 hour. However, there were relative differences in metabolic activity, ALP and BCA. A possible explanation of the difference is the way in which strontium can affect bone cells. Strontium ions affect both proliferation and differentiation pathways, and it is possible that

the proliferation pathway vs the differentiation pathway is stimulated differently in both groups [19, 41]. For example, on day 7 in the 2 hour seeding time group, the amount of cells (BCA) goes up with the strontium release, while ALP activity also increases with strontium ion release. Both pathways here seem to be affected. In the 1 hour seeding time, only seems to go up with increasing strontium concentration in the electrolyte, indicating only effect on the differentiation pathway.

Another possible cause of the difference is simply the increase in the amount of cells. Due to more cells on the implant, it is possible that not all cells have access to strontium ion and thus are not affected by it, or that the cells had no space to differentiate. It is known that a higher cell density influences both the proliferation and the differentiation rate of MSCs [42-44]. Additionally, cell-cell interactions greatly increase proliferation, which could cause the higher protein content in the 2 hour seeding time condition [45]. This could partially explain the differences.

In the research on implants, early differentiation was assessed, but differentiation at a later stage and assessing mineralization of MSCs on strontium incorporated implants will be a crucial part of future results. To investigate these later stage effects, the PEO process must be optimized so the implant material characteristics are similar between the PEO treated implants. If mineralization on strontium incorporated titanium implants is favorable, in vivo studies could become an option along the way.

4.3 Co-culture vs single culture response to strontium

The results of the MSC and EC responses in the co-culture were strikingly different from the earlier single cell type experiments (see section 8.1 Effects of Strontium in medium). In these previously performed studies, strontium increased ALP activity in MSCs and increased metabolic activity in both MSCs and ECs. Earlier research on co-cultures of other bone and endothelial cell lines resulted in improved differentiation of bone cells and improved angiogenesis in endothelial cells [46-48]. However, in the co-culture in this study, these effects were not seen anymore. Apart from the different cell types that were used, a possible cause could be the smaller size of the earlier used well plates and thus more relatively more evaporation of medium. More evaporation of medium could have led to faster differentiation in MSCs and could therefore be the cause. Another difference between the experiments is the use of (empty) transwells in the co-cultures. It is possible that the transwells may have limited the extent of evaporation, which leads to different cell behavior. Further investigation of the cell-cell interactions of ECs and MSCs in co-culture and the influence of strontium on these interactions is needed.

5. Conclusion

In conclusion, strontium is incorporated into the implants and is released while the implants are immersed in fluid. The strontium release diminishes over time and is lower in implants that were made using an electrolyte with a high strontium concentration, most likely due to the differential effects of the ions on the conductance of the implants during the PEO process. This is probably the reason why the lower rate of MSC differentiation in the PT + 1 M Sr implant group.

The incorporation of strontium in implants surfaces could stimulate both proliferation and differentiation of MSCs and this could be the cause of the different cell responses in different groups.

The morphology of the strontium incorporated implants also seem to have an effect: the strontium incorporated implants are favorable compared to PEO treated implants, as cells grow more abundantly on these morphologies as shown by SEM.

Finally, MSCs could improve EC differentiation and angiogenesis in ECs is improved by co-culture with MSCs and by strontium.

6. Acknowledgements

First of all, I would like Dr.ir. Lidy Fratilla-Apachitei, Dr.ir. Iulian Apachitei and Dr.ir. Bram van der Eerden for the opportunity to work on this interesting topic and their guidance and advice throughout this internship. I would also like to thank ir. Ingmar van Hengel for his daily supervision and guidance. Furthermore, I would like to thank Marijke Koedam and Iris Robbesom for their essential help and guidance while I was learning how to work in a biological lab. The experiments would not have been possible without the collaboration with the Bone and Calcium Research group in the Erasmus MC Department of Internal Medicine and the PEO lab of the TU Delfts Department of materials science. The past year has been an amazing experience and I would like to thank all my colleagues at the Bone and Calcium Research group in the Erasmus MC Department of Internal Medicine for improving the experience even more. Next, I would like to deeply thank all my friends and family for their patience and cheerfulness during these few months, especially Thomas, who was there for me at all times.

7. References

1. Wilcock, G.K., *Economic aspects of the demand for total hip replacement in the elderly*. Age Ageing, 1979. **8**(1): p. 32-5.
2. Culliford, D., et al., *Estimating prosthesis survival following total hip replacement in the United Kingdom*. Osteoarthritis and Cartilage. **20**: p. S180-S181.
3. Carr, A.J., et al., *Knee replacement*. Lancet, 2012. **379**(9823): p. 1331-40.
4. Clohisy, J.C., et al., *Reasons for revision hip surgery: a retrospective review*. Clin Orthop Relat Res, 2004(429): p. 188-92.
5. Sheth, N.P., M.B. Bonadio, and M.K. Demange, *Bone Loss in Revision Total Knee Arthroplasty: Evaluation and Management*. J Am Acad Orthop Surg, 2017. **25**(5): p. 348-357.
6. Parithimarkalaignan, S. and T.V. Padmanabhan, *Osseointegration: An Update*. J Indian Prosthodont Soc, 2013. **13**(1): p. 2-6.
7. Stocum, D.L., *Regenerative biology and medicine*. 2012, Elsevier/Academic Press: Amsterdam.
8. Marsell, R. and T.A. Einhorn, *THE BIOLOGY OF FRACTURE HEALING*. Injury, 2011. **42**(6): p. 551-5.
9. Victoria, G., et al., *Bone stimulation for fracture healing: What's all the fuss?* Indian J Orthop, 2009. **43**(2): p. 117-20.
10. Adair TH, M.J., *Angiogenesis*. San Rafael (CA): Morgan & Claypool Life Sciences.
11. Knight, S.R., R. Auja, and S.P. Biswas, *Total Hip Arthroplasty - over 100 years of operative history*. Orthop Rev (Pavia), 2011. **3**(16): p. 3.
12. Lütjering, G. and J.C. Williams, *Titanium*. Engineering Materials and Processes. 2003, Berlin; New York: Springer-Verlag Berlin Heidelberg. 379.
13. Zhu, X., K.-H. Kim, and Y. Jeong, *Anodic oxide films containing Ca and P of titanium biomaterial*. Biomaterials, 2001. **22**(16): p. 2199-2206.
14. Palmquist, A., et al., *Titanium oral implants: surface characteristics, interface biology and clinical outcome*. Journal of the Royal Society, Interface, 2010. **6**(7, Supplement 5): p. 13.
15. Kilpadi, D.V., et al., *Cleaning and heat-treatment effects on unalloyed titanium implant surfaces*. Int J Oral Maxillofac Implants, 2000. **15**(2): p. 219-30.
16. Yang, Y., et al., *Enhancing osseointegration using surface-modified titanium implants*. JOM, 2006. **58**(7): p. 71-76.
17. Marie, P.J., *Strontium ranelate: New insights into its dual mode of action*. Bone, 2007. **40**(5, Supplement 1): p. S5-S8.
18. Thomsen, A.R., et al., *Strontium is a biased agonist of the calcium-sensing receptor in rat medullary thyroid carcinoma 6-23 cells*. J Pharmacol Exp Ther, 2012. **343**(3): p. 638-49.
19. Zhang, W., et al., *A strontium-incorporated nanoporous titanium implant surface for rapid osseointegration*. Nanoscale, 2016. **8**(9): p. 5291-5301.
20. van Hengel, I.A.J., et al., *Data on the surface morphology of additively manufactured Ti-6Al-4V implants during processing by plasma electrolytic oxidation*. Data Brief, 2017. **13**: p. 385-389.
21. Athanasiadis, S., *Osteogenic and antibacterial activity of strontium and silver containing additively manufactured titanium implants*, in *Department of Biomechanical Engineering*. 2016, Technical University of Delft: Delft. p. 47.
22. Edgell, C.J., C.C. McDonald, and J.B. Graham, *Permanent cell line expressing human factor VIII-related antigen established by hybridization*. Proc Natl Acad Sci U S A, 1983. **80**(12): p. 3734-7.
23. Fisher, T. *Hoehst 33342, Trihydrochloride, Trihydrate, 100 mg*. Hoehst 33342, Trihydrochloride, Trihydrate, 100 mg 2018 [cited 2018 05/23/18]; Available from: <https://www.thermofisher.com/order/catalog/product/H1399>.
24. Fisher, T. *Propidium Iodide*. Propidium Iodide 2018 [cited 2018 05/23/18]; Available from: <https://www.thermofisher.com/order/catalog/product/H1399>.

25. Martín-Navarro, C.M., et al., *PrestoBlue® and AlamarBlue® are equally useful as agents to determine the viability of Acanthamoeba trophozoites*. *Experimental Parasitology*, 2014. **145**: p. S69-S72.
26. Bacabac, R.G., et al., *Round versus flat: Bone cell morphology, elasticity, and mechanosensing*. *Journal of Biomechanics*, 2008. **41**(7): p. 1590-1598.
27. Abhinand, C.S., et al., *VEGF-A/VEGFR2 signaling network in endothelial cells relevant to angiogenesis*. *J Cell Commun Signal*, 2016. **10**(4): p. 347-54.
28. Behera, J., et al., *MUC1 in osteoblasts balances osteogenesis and angiogenesis under hypoxia*, in *4th Joint Meeting of ECTS and IBMS*. 2015: Rotterdam.
29. Knowles, H.J., et al., *Hypoxia-inducible factor regulates osteoclast-mediated bone resorption: role of angiopoietin-like 4*. *Faseb j*, 2010. **24**(12): p. 4648-59.
30. Krock, B.L., N. Skuli, and M.C. Simon, *Hypoxia-Induced Angiogenesis: Good and Evil*. *Genes Cancer*, 2011. **2**(12): p. 1117-33.
31. Fuoss, R.M., *Conductance of Dilute Solutions of 1-1 Electrolytes*. *Journal of the American Chemical Society*, 1959. **81**(11): p. 2659-2662.
32. Wen, J., et al., *Strontium delivery on topographical titanium to enhance bioactivity and osseointegration in osteoporotic rats*. *J. Mat. Chem. B*, 2015. **3**(24): p. 4790-4804.
33. Zhou, J. and L. Zhao, *Multifunction Sr, Co and F co-doped microporous coating on titanium of antibacterial, angiogenic and osteogenic activities*. *Sci. rep.*, 2016. **6**: p. 14.
34. Yuan, X., et al., *Immunomodulatory effects of calcium and strontium co-doped titanium oxides on osteogenesis*. *Front Immunol*, 2017. **8**: p. 15.
35. Yu, J.M. and H.C. Choe, *Morphology changes and bone formation on PEO-treated Ti-6Al-4V alloy in electrolyte containing Ca, P, Sr, and Si ions*. *Appl Surf Sci*, 2017: p. 10.
36. He, X., et al., *Antibacterial ability and osteogenic activity of porous Sr/Ag-containing TiO₂ coatings*. *Biomed Mater*, 2016. **10**(11): p. 4.
37. Liu, Y.T., et al., *Engineering three-dimensional structures using bio-inspired dopamine and strontium on titanium for biomedical application*. *J. Mat. Chem. B*, 2014. **2**(45): p. 7927-7935.
38. Chung, C.J. and H.Y. Long, *Systematic strontium substitution in hydroxyapatite coatings on titanium via micro-arc treatment and their osteoblast/osteoclast responses*. *Acta Biomater*, 2011. **7**(11): p. 4081-4087.
39. Fatimah, S., et al., *Dual incorporation of SiO₂ and ZrO₂ nanoparticles into the oxide layer on 6061 Al alloy via plasma electrolytic oxidation: Coating structure and corrosion properties*. *Journal of Alloys and Compounds*, 2017. **707**: p. 358-364.
40. Schumacher, M., et al., *A novel strontium(II)-modified calcium phosphate bone cement stimulates human-bone-marrow-derived mesenchymal stem cell proliferation and osteogenic differentiation in vitro*. *Acta Biomaterialia*, 2013. **9**(12): p. 9547-9557.
41. Bose, S., et al., *Understanding of dopant-induced osteogenesis and angiogenesis in calcium phosphate ceramics*. *Trends in Biotechnology*, 2013. **31**(10): p. 594-605.
42. Fossett, E. and W.S. Khan, *Optimising Human Mesenchymal Stem Cell Numbers for Clinical Application: A Literature Review*. *Stem Cells Int*, 2012. **2012**.
43. Eyckmans, J., G.L. Lin, and C.S. Chen, *Adhesive and mechanical regulation of mesenchymal stem cell differentiation in human bone marrow and periosteum-derived progenitor cells*. *Biol Open*, 2012. **1**(11): p. 1058-68.
44. Takagi, M., et al., *High inoculation cell density could accelerate the differentiation of human bone marrow mesenchymal stem cells to chondrocyte cells*. *J Biosci Bioeng*, 2007. **103**(1): p. 98-100.

45. Mousavi, S.J. and M.H. Doweidar, *Role of Mechanical Cues in Cell Differentiation and Proliferation: A 3D Numerical Model*. PLoS One, 2015. **10**(5): p. e0124529.
46. Sammons, R., *3 - Biological responses to hydroxyapatite*, in *Hydroxyapatite (Hap) for Biomedical Applications*, M. Mucalo, Editor. 2015, Woodhead Publishing. p. 53-83.
47. Unger, R.E., et al., *Tissue-like self-assembly in cocultures of endothelial cells and osteoblasts and the formation of microcapillary-like structures on three-dimensional porous biomaterials*. Biomaterials, 2007. **28**(27): p. 3965-76.
48. Dariima, T., et al., *Cooperation between osteoblastic cells and endothelial cells enhances their phenotypic responses and improves osteoblast function*. Biotechnol Lett, 2013. **35**(7): p. 1135-43.

8. Appendix

8.1 Effects of Strontium in medium

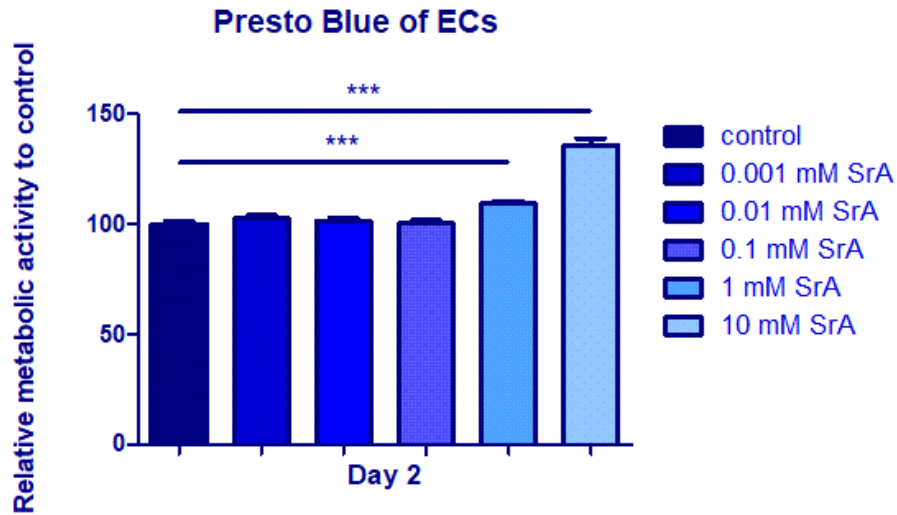


Figure 20: Presto Blue of ECs with various concentrations of strontium with strontium in medium

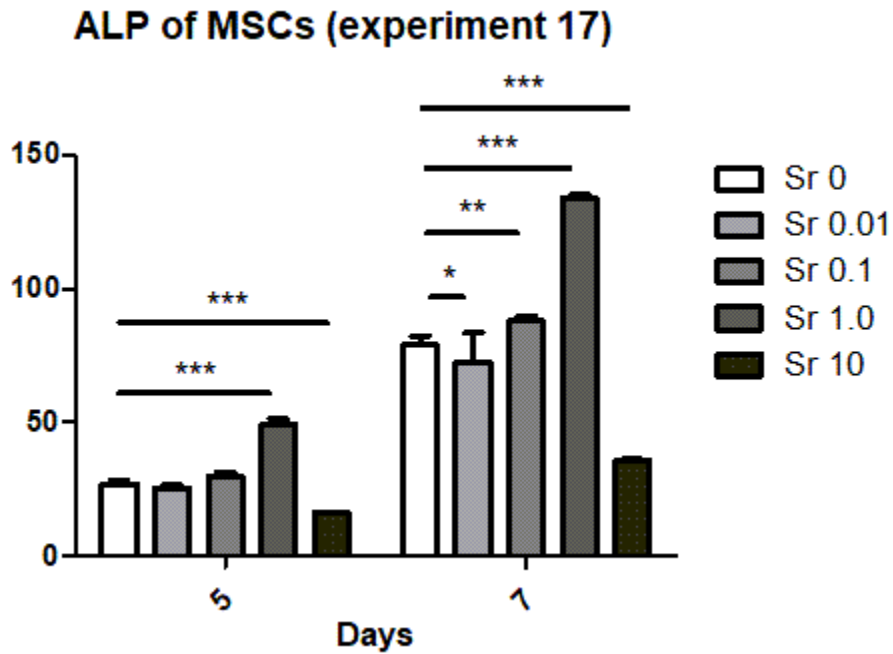


Figure 21: ALP of MSCs with various concentrations of strontium with strontium in medium

Presto Blue of MSCs (experiment 17)

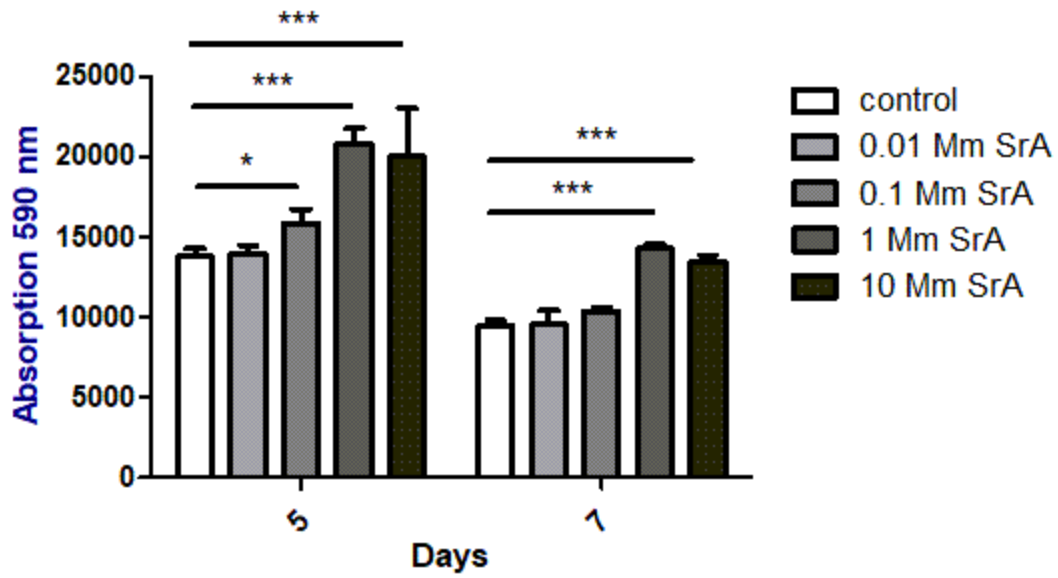


Figure 22: Presto Blue of MSCs with various concentrations of strontium with strontium in medium

8.2 Effect of ECM coating of implants of MSCs

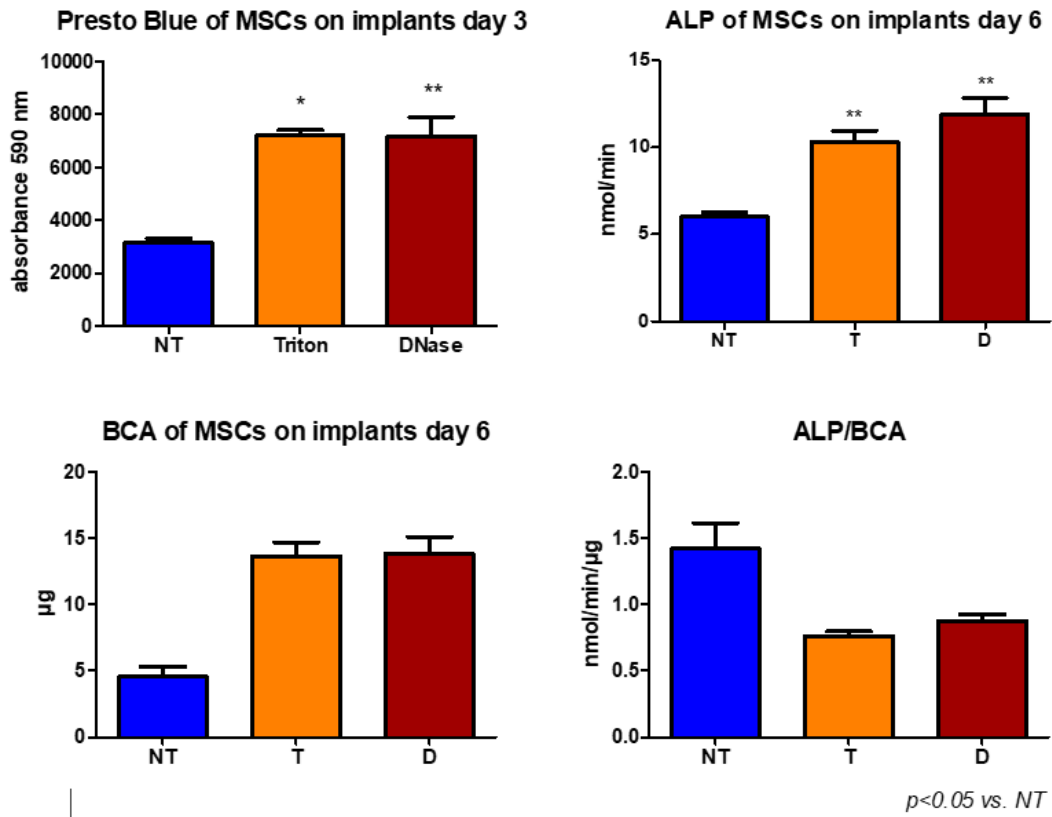


Figure 23: Presto Blue, ALP and BCA of MSCs on implants, NT = non treated, T = non treated coated with triton-extracted ECM, D = NT coated with DNase extracted ECM

8.3 SEM images of MSCs on implants

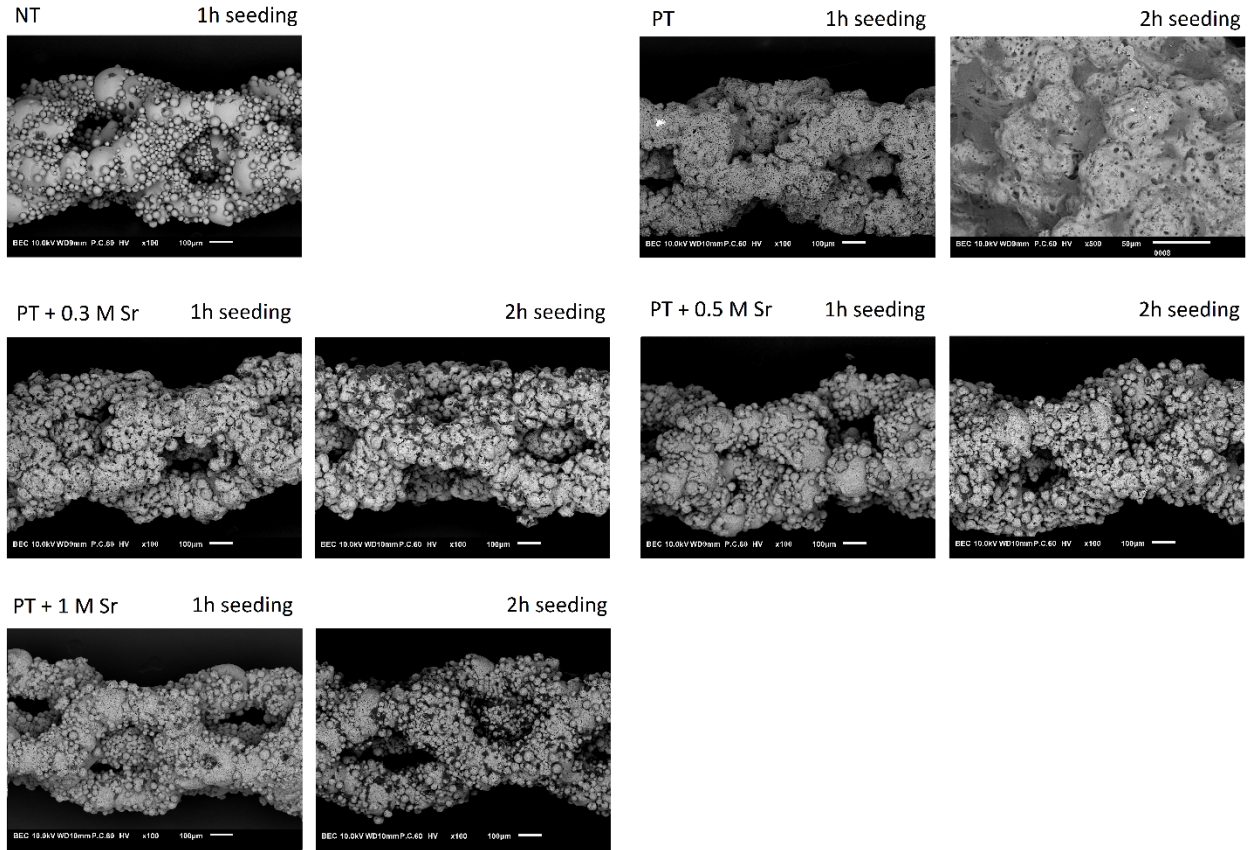


Figure 24: MSCs on implants with 1 vs 2 hour seeding on day -2 (NT 2h seeding not available)

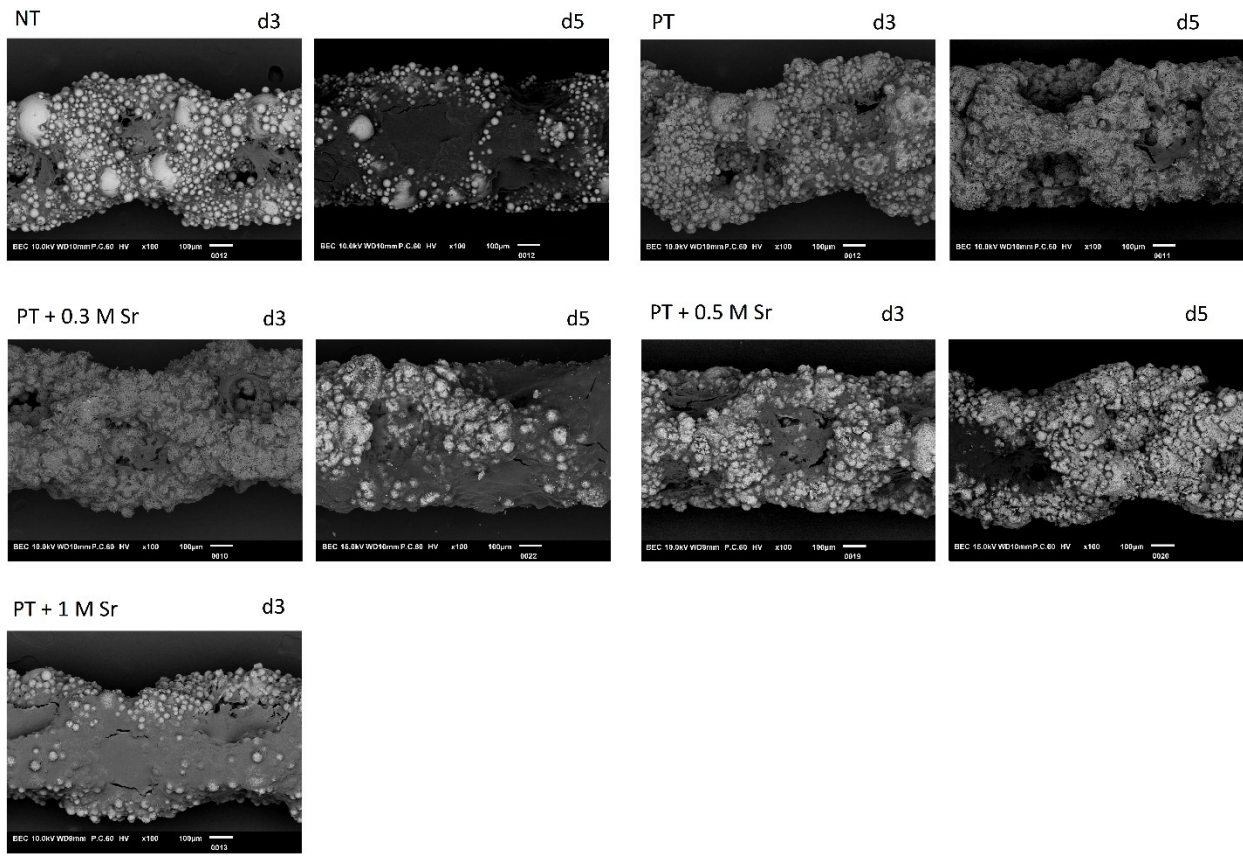


Figure 25: MSCs on implants with 2 hour seeding time on day 3 and day 5 (PT + 1 M Sr day 5 not available)

8.4 Release of strontium in molars

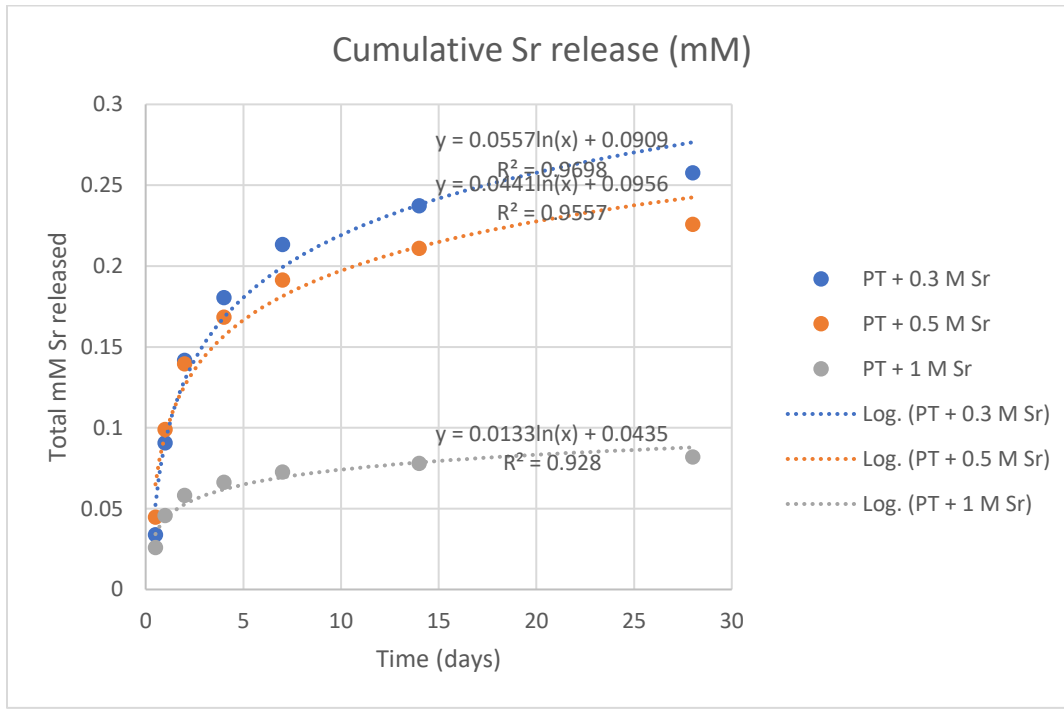


Figure 26: Cumulative Sr ion release profile for the implant groups (n=3) in mM

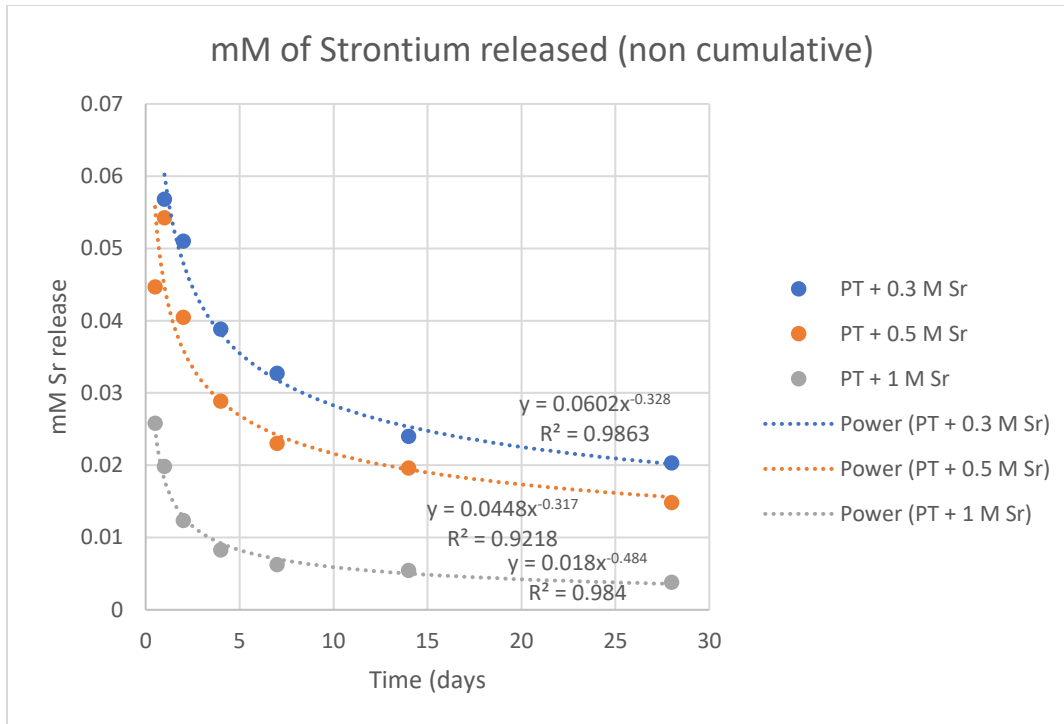


Figure 27: Non-cumulative Sr ion release profile for the implant groups (n=3) in mM

8.5 Primer sequences for PCR

Gene	Primer For pmol/reactie	primer Rev pmol/reactie	Forward primer (5'-3')	Reverse primer (5'-3')
GAPDH	2,5	2,5	CCGCATCTTCTTTTGCCTCG	CCCAATACGACCAAATCCGTTG
HIF1A	2,5	2,5	GAGGGAGCCAGCGCTTAG	ACTTATCTTTTCTTGTGCTTCGC
MUC1	5	5	AGTGCTTACAGTTGTTACGGGT	GCTGGGCACTGAACTTCTCT
VEGF-A1	5	5	ACAACAAATGTGAATGCAGACCA	TACCGGGATTCTTGCCTT